

**MEASUREMENT OF RADON EXHALATION AND ITS
MODELING ALONG KURLOK FAULT REGIONS OF KOLASIB
DISTRICT, MIZORAM**

**A THESIS SUBMITTED IN PARTIAL FULFILLMENT OF THE
REQUIREMENTS FOR THE DEGREE OF DOCTOR OF
PHILOSOPHY**

LALDINGNGHETA RALTE

MZU REGISTRATION NO: 1567 of 2009-10

Ph.D REGISTRATION NO: MZU/Ph.D/1003 of 15.05.2017



**DEPARTMENT OF PHYSICS
SCHOOL OF PHYSICAL SCIENCE
SEPTEMBER, 2022**

**MEASUREMENT OF RADON EXHALATION AND ITS
MODELING ALONG KURLOK FAULT REGIONS OF KOLASIB
DISTRICT, MIZORAM**

By

Laldingngheta Ralte

Department of Physics

Name of Supervisor: Prof. R.C.Tiwari

Name of Joint Supervisor: Dr. Rosangliana

**Submitted
in partial fulfillment of the requirement of the
Degree of Doctor of Philosophy
in Physics of Mizoram University, Aizawl**



Prof.R.C Tiwari
Senior Professor

Mizoram University
Department of Physics
(A DST-FIST Supported
Department)
School of Physical Sciences
Aizawl 796 004 Mizoram
E-mail : ramesh_mzu@rediffmail.com
Phone: 9862300514

Date: 20th September 2022

Certificate

This is to certify that the thesis entitled '*Measurement of Radon exhalation and its modeling along Kurlok Fault regions of Kolasib District, Mizoram*', submitted by Shri Laldingngehta Ralte, for the degree of Doctor of Philosophy of the Mizoram University, Aizawl, embodies the record of original investigations carried out by him under my supervision. The thesis presented is worthy of being considered for the award of Ph. D. degree. This work has not been submitted for any degree to any other University.

(Prof. RAMESH CHANDRA TIWARI)

Supervisor

(Dr. ROSANGLIANA)

Jt. Supervisor

Declaration
Mizoram University
September, 2022

*I, **Laldingngheta Ralte**, hereby declare that the subject matter of this thesis is the record of work done by me, that the contents of this thesis did not form basis of the award of any previous degree to me or to the best of my knowledge to anybody else, and that the thesis has not been submitted by me for any research degree in any other University or Institute.*

This is being submitted to the Mizoram University for the degree of Doctor of Philosophy in Physics.

(LALDINGNGHETA RALTE)

Candidate

(Prof. ZAITHANZAUVA PACHUAU)

Head

(Prof. RAMESH CHANDRA TIWARI)

Supervisor

Acknowledgment

I would like to express my gratitude to my Supervisor Prof. R.C Tiwari, Department of Physics, Mizoram University, for his valuable guidance and supervision throughout the course of my work.

I would also like to express my sincere gratitude to my Joint Supervisor Dr. Rosangliana, Department of Physics, Govt. Zirtiri Residential Science College, who helped me in every step of the work involved in the thesis and his guidance throughout the completion of this work.

I express my heartfelt thanks to Prof. Diwakar Tiwari, Dean, School of Physical Sciences for his support in the completion of my work. I would also like to thank the Teaching and non-Teaching Faculties of the Department of Physics, Mizoram University for guidance and valuable advice during my progress reports.

I would also like to thank Dr. B.K. Sahoo and his team from Radiological Physics and Advisory Division, Bhabha Atomic Research Centre, Mumbai, for training us for the project works and for their hospitality during our training in Mumbai. I would like to thank my colleagues Dr. Hmingchungnunga and Dr. Vanramlawma, Department of Physics, Mizoram University and Mr. Simon Lalremruata for their valuable time and assistance in the completion of this work. I would also like to thank Dr. Lawrence Zonunmawia Chhangte, Govt. Zirtiri Residential Science College for sharing me his valuable knowledge in the subject.

I am indebted to my parents and family members for their encouragement and moral support during the course of my studies. Above all else, I thank the Lord Almighty for being with me throughout these years and keeping me in good health to complete this work.

Dated: 20th September, 2022

Department of Physics,
Mizoram University, Aizawl.

(LALDINGNGHETA RALTE)

CONTENTS

	Pages
Title of the Thesis	i
Certificates	ii
Declaration	iii
Acknowledgement	iv
Contents	v
List of Figures	viii
List of Tables	x
Dedication	xi
CHAPTER 1 : Introduction	
1.1 : Natural Radioactivity	1
1.2 : Ionizing Radiation	1
1.3 : Uranium	3
1.4 : Thorium	6
1.5 : Potassium	8
1.6 : Radon	8
1.6.1 : Health effects of Radon	10
1.6.2 : Radon in soil	11
1.6.3 : Measurement Techniques	13
1.7 : Smart RnDuo	15
1.8 : Faults	17
1.9 : Review of literature	19
CHAPTER 2 : Theory and Methodology	
2.1 : Smart RnDuo	24
2.1.1 : Smart RnDuo for measurement of radon mass exhalation rate from soil	27
2.1.2 : Modeling of exhalation rate with measured and calculated values	30

2.1.3	:	Measurement of Radon in soil gas using soil probe	31
2.2	:	Gamma Spectrometry Using NaI(Tl) Detector	31
2.2.1	:	Efficiency and Energy Calibration of NaI(Tl) Detector	34
2.2.2	:	Activity Concentration Measurement	36
2.2.3	:	Determination of Radium Equivalent Activity And Hazard Indices	37
2.5	:	Spot Background Gamma Detection	38
2.6	:	Soil Type and Grain Size Determination	40
CHAPTER 3	:	Determination of Radon Mass Exhalation Rate, Radon Concentration in Soil Gas and Soil Grain Size Distribution	
3.1	:	Measurement of radon mass exhalation rate	42
3.1.2	:	Results and Discussion	43
3.1.1	:	Modeling of Radon Exhalation	46
3.2	:	Measurement of radon concentration in soil gas	50
3.2.1	:	Results and Discussion	51
3.3	:	Soil Type Determination	55
3.3.1	:	Results and Discussion	56
CHAPTER 4	:	Experimental Determination Natural Radioactivity and Radon Mass Exhalation Rate in Soil and Measurement of Spot Background Gamma Radiation	
4.1	:	Determination of Natural Radioactivity in Soil	59
4.1.1	:	Results and Discussions	60

4.2	:	Estimation of Radium Equivalent Activity	61
4.3	:	Estimation of external and internal hazard indices	63
4.4	:	Spot Background Gamma Radiation	64
4.4.1	:	Results and Discussions	64
4.5	:	Correlation between Background Gamma and Radium Equivalent Activity	67
CHAPTER 5	:	Conclusion	69
Appendices	:	Appendix – I	74
		Appendix – II	75
		Appendix – III	76
		Appendix – IV	77
		Appendix – V	78
References	:		80
Brief bio-data of the author	:		88
Publications and activities:			90
Particulars of Candidate	:		93

Lists of Figures

Figure No.	Titles of the Figures	Page
1.1	^{238}U Decay Series	5
1.2	^{232}Th Decay Series	7
1.3	Movement of radon in soil	13
1.4	Schematic of radon measurement process in RnDuo	16
1.5	Geographical map of study area with fault lines	18
2.1	Sampling areas of Kolasib District	24
2.2	Schematic diagram of Smart RnDuo	25
2.3	Measurement of Radon Mass Exhalation Rate using Smart RnDuo	28
2.4	Mass Exhalation Chamber	29
2.5	Measurement of Radon concentration in soil gas using Smart RnDuo	31
2.6	Initial settings of multi-channel analyzer	33
2.7	NaI Detector connected with GSPEC-SA	34
2.8	IAEA Standard Sources for Energy and Efficiency Calibration	36
2.9	Gamma Survey Meter PM 1405	39
2.10	Mechanical Sieve Shaker	41
3.1	Geological map of the study area for mass exhalation	43
3.2	Radon mass exhalation from fault regions of Kolasib District.	46
3.3	Comparison figure of measured and calculated exhalation rates.	47
3.4	Geographical map of measured and calculated exhalation rate.	48
3.5	Radon concentration in soil gas at different depths	53
3.6	Average radon concentration in soil gas at different depths	53

3.7	USDA triangular plot for soil samples from Kolasib District	57
4.1	Geographical map for natural radioactivity mesurment.	59
4.2	Graph of Activity Concentrations of ^{238}U , ^{232}Th and ^{40}K radionuclide in soil samples collected from fault regions of Kolasib District	61
4.3	Radium equivalent activity concentration in soil samples collected from fault regions of Kolasib District.	63
4.4	External and internal hazard indices of ^{238}U , ^{232}Th and ^{40}K radionuclide in soil samples collected from fault regions of Kolasib District.	64
4.5	Background gamma radiation for fault regions of Kolasib district.	66
4.6	Background gamma radiation for only Kurlok fault regions	67
4.7	Correlation between background gamma level and radium equivalent activity in fault regions of Kolasib District.	68

Lists of Tables

Table No.	Title of the Table	Page
1.1	Physical Properties of radon	10
2.1	Technical specifications of Smart RnDuo	26
3.1	Measurement of radon mass exhalation from fault regions of Kolasib district	44
3.2	Comparison table of measured and calculated exhalation rates.	47
3.3	Measurement of radon mass exhalation from fault regions of Aizawl district	49
3.4	Radon concentration in soil gas at different depths	52
3.5	Comparison of radon concentration of this present study with other investigators	53
3.6	Determination of soil grain size from fault regions of Kolasib District	56
4.2	Activity Concentrations of ^{238}U , ^{232}Th and ^{40}K radionuclide in soil samples collected from fault regions of Kolasib District	60
4.3	Radium equivalent activity, External and internal hazard indices of ^{238}U , ^{232}Th and ^{40}K radionuclide in soil samples collected from fault regions of Kolasib District	62
4.4	Background gamma radiation for fault regions of Kolasib district.	64

***THIS THESIS
IS DEDICATED
TO
MY FATHER LALRAMHLUNA
AND
MY MOTHER LALRAMNGHAKI***

INTRODUCTION

1.1 Natural Radioactivity:

Radiation, also known as radiant energy, is energy that travels through space in the form of waves or particles. Radioactive decay is a feature of various elements that occurs naturally as well as element isotopes that are created artificially. The half-life of a radioactive element is defined as the time it would take for half of any given quantity of the isotope to disintegrate. Radioactive decay occurs when naturally occurring radionuclides dissolve into their daughter elements or progenies, emitting ionising radiation in the form of alpha, beta, or gamma radiations. The daughter element or progenies dissolve further into other radioactive elements until they reach a stable state, establishing a decay chain. Natural radiation sources account for around 87 percent of a human's radiation exposure, with manmade radiation accounting for the remaining 13 percent (Kannan *et al.*, 2002).

Radiation is classified as either ionising or non-ionizing based on how it interacts with matter. Ionizing radiation ionises atoms by 'knocking' electrons off of them, changing the chemical state of matter and causing biological damage as a result. Without displacing electrons, non-ionizing radiation bounces off or passes through matter.

1.2 Ionizing radiation:

(a) Alpha radiations: Helium nuclei with positively charged particles make up alpha radiations. Because alpha decay radiation has a low penetrating power, it cannot penetrate human skin or even a thin sheet of paper, and is therefore considered externally safe. If alpha emitting radionuclides are consumed or inhaled, however, they can harm the body's internal organs, particularly the lungs, stomach, and kidneys.

(b)Beta radiation: It is from radioactive decay of heavy nuclei might entail electron emission, positron emission, or electron capture, depending on the mechanism of decay. A nucleus with an excess neutron produces an electron and anti-neutrino in electron emission. When a nucleus has an excess proton, it produces a positron and a neutrino, which is known as positron emission. The excess positive charge of the nucleus can sometimes be neutralised by the capture of an orbital electron in heavy nuclei, where electron orbits are closely packed and considerably closer to the nucleus. This process is known as electron capture. Beta radiation has a penetrating power that is halfway between alpha and gamma, and it can be blocked by a few millimetres of aluminium sheet.

(c)Gamma Radiation: The emission of gamma radiation is invariably followed by the emission of alpha or beta particles from naturally occurring radionuclides. When a radioactive substance emits alpha or beta particles, the daughter nucleus may be in one or more excited states. The nucleus produces high-energy photons in the form of gamma radiations as it transitions from an excited state to the ground state or from a higher excited state to a lower excited one. Gamma rays have a strong penetrating power and can easily permeate the body, causing harm to human cells. However, they can be prevented by a lead or concrete block.

Man-made/artificial ionising radiation and natural ionising radiation are the two types of ionising radiation. Man-made ionising radiation makes up a small percentage of total ionising radiation, which is known as Background Radiation. This background radiation is, in reality, the primary source of radiation in the environment. Background radiation is largely consistent over time and is present in the environment now in the same amounts as it was many years ago. Depending on the source, background radiation is classified as cosmic, terrestrial, or internal.

Cosmic radiation is a type of space radiation that is constantly impacting the Earth. The Sun and other stars in our galaxy release a continuous stream of cosmic radiation. Because cosmic radiation is somewhat shielded by the atmosphere, the strength of this radiation is proportional to altitude above sea level. The magnetic shield around the Earth shields us from cosmic radiation, and it is highest near the

equator and weakest towards the poles. Most of the radiation is diverted around the earth by the magnetic shield. The majority of the remaining radiation that travels to Earth is shielded by Earth's atmosphere. The elevation at which we reside determines a portion of our cosmic radiation exposure.

Radionuclides in the environment cause internal radiation, which enters the body through the air we breathe and the food we eat. They can also get in through a wound that is open. Isotopes of uranium and its progeny, particularly radon (^{222}Rn) and its progeny, thoron (^{220}Rn) and its progeny, potassium (^{40}K), rubidium (^{87}Rb), and carbon are natural radionuclides that can be inhaled and consumed (^{14}C). The most common radionuclides found in the human body are ^{40}K and ^{210}Po ; additional radionuclides include rubidium (^{87}Rb) and carbon (^{14}C).

The decay of radioactive elements in the ground produces terrestrial external radiation. The natural breakdown or radioactive decay of radioisotopes in natural materials such as rocks, soil, vegetation, and groundwater produces terrestrial external radiation. Radioactive decay is a natural occurrence that has occurred since the dawn of time. Humans are exposed to radiation directly from radioactive minerals in the earth. The global average natural radiation dose to humans is approximately 0.3 - 0.6 mSv/year, which is four times greater than the global average of artificial radiation exposure, later increased to 0.3 – 1.0 mSv/year in the year 2008 (UNSCEAR 2000, UNSCEAR 2008)

1.3 Uranium:

Uranium has been a plentiful source of concentrated resources for over 60 years. It is found in most rocks in quantities of 2 to 4 parts per million and is as common in the earth's crust as nickel, tungsten, and molybdenum. Martin Klaproth, a German chemist, discovered the element in the mineral Pitchblende in 1789. It was given the name Uranus after the planet Uranus. Uranium is the heaviest trace element found in all terrestrial compounds at varying concentrations. Natural uranium is found in different proportions in rocks and soil, and due to the low density of their oxides, they are concentrated on the earth's crust rather than the mantle or core. Pitchblende, a key ingredient of igneous rocks, granites, and pegmatite, is the

principal mineral source of uranium. Natural uranium has three isotopes that are all radioactive in nature: ^{238}U , ^{235}U , and ^{234}U . Among the three natural uranium isotopes, ^{238}U is the most plentiful, accounting for more than 99 percent of total uranium present in nature. The abundance of ^{238}U in nature makes it an interesting isotope, and its concentration and distribution in soils, rocks, and water could have a negative impact on human health. Furthermore, ^{238}U is the parent element of the most hazardous and investigated radon isotope, ^{222}Rn . Many Indian researchers from various regions in India reported the activity concentration of Uranium and Thorium (Kalyani *et al.*, 1990; Rekhakutty *et al.*, 1993; Kumar *et al.*, 2003; Mahur *et al.*, 2008; Kerur *et al.*, 2011; Manjunatha *et al.*, 2013; Amit Kumar *et al.*, 2014)

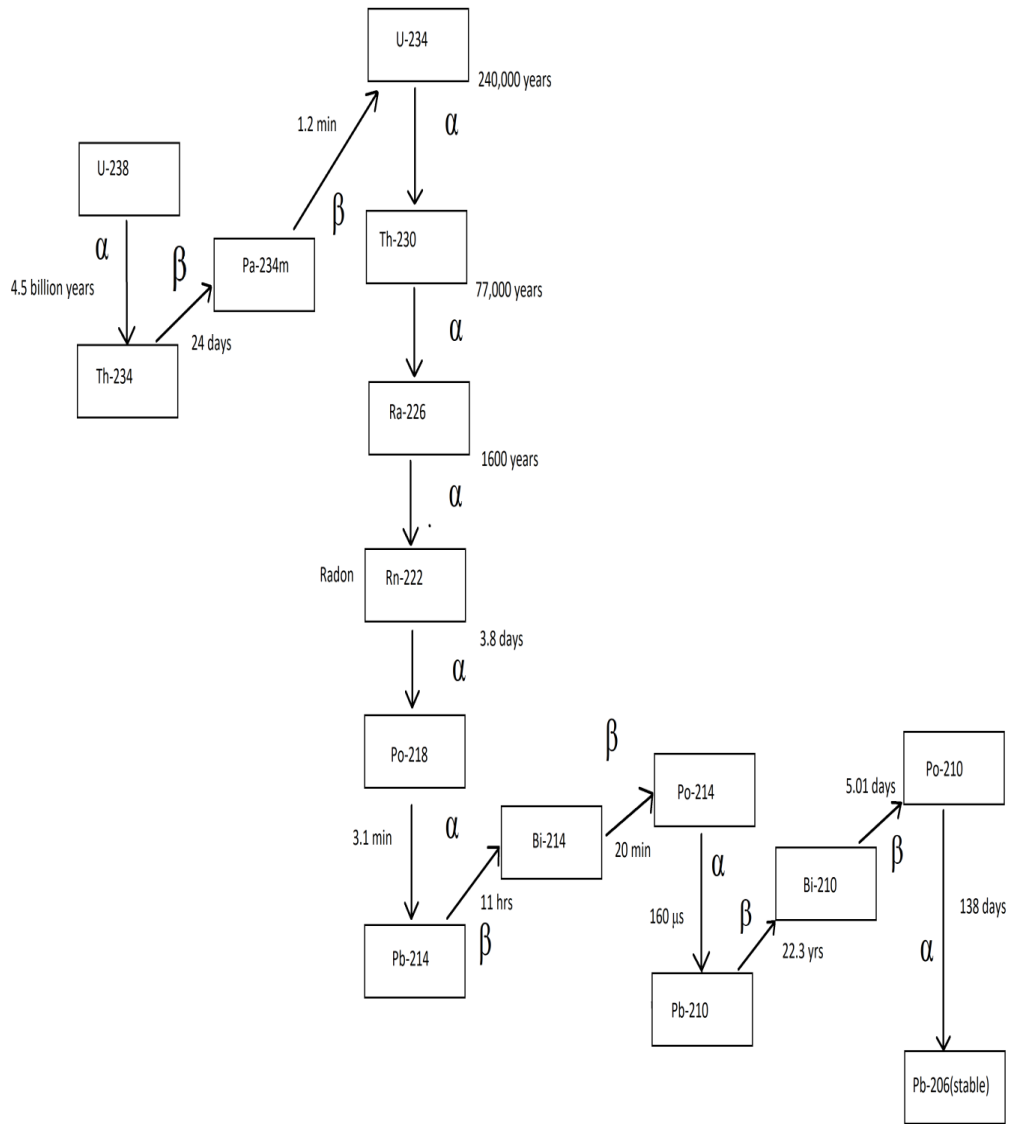


Figure 1.1: ^{238}U Decay Series

1.4 Thorium:

Jöns Jacob Berzelius, a Swedish scientist, discovered thorium in 1828. When exposed to air, it turns silvery white but grey or black. It is around half the abundance of lead and three times the abundance of uranium in the Earth's crust. Thorium is extracted commercially from the mineral monazite, although it can also be found in other minerals such as thorite and thorianite. So far, 31 thorium isotopes with mass numbers ranging from 208 to 238 have been found. All thorium isotopes are radioactive, and of the 31 known thorium isotopes, ^{232}Th is the most stable, with a half-life of 14.05 billion years, and is the only primordial isotope of thorium. Furthermore, ^{232}Th accounts for virtually all of the thorium found on Earth. The global average for thorium concentration in soil is 45 Bq/kg, while the Indian average is 18.36 Bq/kg (UNSCEAR 2000, 2008). The abundance of thorium in nature is comparable to that of lead, and it accounts for around 0.0002–0.001% of the Earth's crust. Thorium is found in igneous rocks such as granites, pegmatites, and gneisses. However, unlike lead, thorium and its compounds are not subjected to the same hydrothermal reactions that result in vast, concentrated mineral deposits. Although thorium concentrations in igneous rocks are rarely greater than 1%, natural processes such as erosion can create isolated deposits of higher thorium concentrations in the form of monazite, which contains roughly 3–10% thorium. People are exposed to thorium mostly through inhalation, intravenous injection, ingestion, and skin absorption. Despite the fact that thorium is abundant in the environment, most people are not exposed to harmful levels of the metal. People who live near thorium-mining areas or facilities that manufacture thorium-containing products, on the other hand, may be more exposed, especially if their water comes from a private well. Inhaling thorium dust has been linked to an increased risk of lung and pancreatic cancer, according to study. Individuals who have been exposed to thorium are also at a higher risk of developing bone cancer because thorium can be retained in bone. According to research, the largest concentrations of thorium were detected in the human body's pulmonary lymph nodes and lungs (Ibrahim *et al.*, 1983; Wrenn *et al.*, 1981; Shashikumar, 2010)

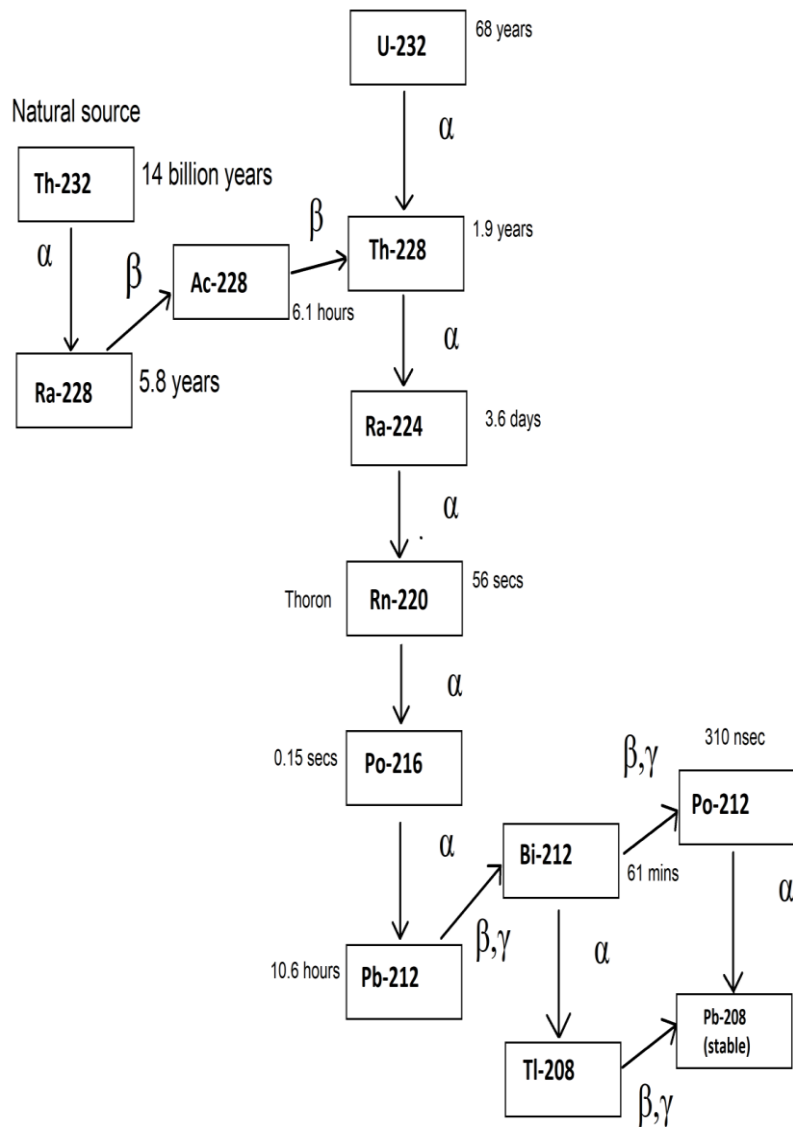


Figure 1.2: ^{232}Th Decay Series

1.5 Potassium:

Natural potassium has three isotopes, two of which are stable and non-radioactive, namely ^{39}K and ^{41}K . One isotope of natural potassium ^{40}K is radioactive, and it accounts for up to one tenth of the potassium found in nature. ^{40}K can be found at various amounts practically everywhere, including human and animal tissues, soils, and oceans. The United Nations Scientific Committee on the Effects of Atomic Radiation (UNSCEAR) concluded in 2000 that the amount of potassium in Indian soils varies from 9 Bq/kg to 572 Bq/kg, with an average value of 369.6 Bq/kg for normal background areas, and from 24Bq/kg to 1362 Bq/kg for high background areas. The current global average value in soil is 412 Bq/kg (UNSCEAR, 2008), which is quite near to the previously prescribed global average value of 400 Bq/kg (UNSCEAR, 2000).

With a half-life of 1.3 billion years, ^{40}K decays using one of two processes: approximately 89 percent of the time, it decays to ^{40}Ca by emitting a beta particle with no accompanying gamma radiation, and approximately 11 percent of the time, it decays to ^{40}Ar by electron capture with emission of an energetic gamma ray. Strong gamma radiation is emitted during the electron-capture decay process, making external exposure to this isotope hazardous to one's health.

Internally, ^{40}K is known to provide a health risk because to radiations emitted by both beta particles and gamma rays. It is easily absorbed into the bloodstream and dispersed throughout the body after consumed. The health risk of ^{40}K is connected with cell damage induced by ionising radiation, which has the potential to cause cancer (Peterson *et al.*, 2001).

1.6 Radon:

Natural Occurring Radionuclide Materials (NORM) are radionuclides that are known to exist in soil and rocks. The natural radionuclides of concern are mostly ^{238}U , ^{232}Th , and ^{40}K . (Hussain *et al.*, 2009).The largest source of natural radiations in the earth's surroundings is natural radioactivity resulting from the ^{238}U decay series. ^{222}Rn is the single most important source of natural radiations among the daughter

elements of ^{238}U because it is constantly generated in the soil and emitted into the earth's atmosphere. Radon was discovered by Friedrich Ernst Dorn while studying the decay chain of radium in 1900. The name is derived from radium, as it was first detected as an emission from radium during radioactive decay. It was firstly named niton from the Latin word “nitens” which means shining, and the name radon was officially given in 1923. Radium was in great demand for treatment of cancer and was quite expensive. Radon gas which is a natural decay of radium was believed to possess similar properties to radium in treatment of cancer. So studies regarding radon gas and its progenies have been conducted ever since its discovery. Several research and studies have been going on in the United States of America for a long period of time.

Radon is a radioactive, colourless, odourless, tasteless noble gas with an atomic radius of 1.34 that occurs naturally as a decay product of Radium (^{226}Ra) along the Uranium (^{238}U) Decay Series. It is the heaviest member of the rare gas group (roughly 100 times heavier than hydrogen and about 7.5 times heavier than air) and stays a gas under normal conditions. Because of its noble nature, radon is chemically neutral to reactions with other gases, allowing it to pass freely through cracks and fractures in rocks and soils, releasing itself into the atmosphere. The fourteen-step sequence of ^{238}U radioactive decay series produces gaseous radon, and the sequence concludes with the synthesis of ^{206}Pb , which is stable and non-radioactive. Radon is water-soluble and has numerous isotope forms, two of which are present in substantial proportions in the human environment — Radon $\text{Rn}222$ and Thoron $\text{Rn}220$. The half-life of this mobile radon isotope 222 is 3.8 days, which is long enough for it to diffuse into the atmosphere through the solid rock or soil in which it is created. More than 25 radon isotopes have been found, with ^{222}Rn (Radon), ^{220}Rn (Thoron), and ^{219}Rn (Actinon) occurring in nature as members of the uranium, thorium, and actinium series, respectively. Thoron has half-life of 55secs and Actinon has half-life of only 4secs. Because of this Actinon series is of minor importance. Table 1.1 shows the physical properties of radon.

Table 1.1:Physical Properties of Radon

Sl. No.	Properties	Values
1	Atomic Radius	1.34 Å
2	Atomic Volume	50.5 cm ³ /mol
3	Molar Volume	50.5 cm ³ /mol
4	Mean Excitation Energy	794.0 eV
5	Melting Point	-71 °C
6	Boiling Point	-61.85 °C
7	Critical Point	377 K at 6.28 MPa
8	Critical Temperature	104 °C
9	Critical Pressure	62 atm.
10	Heat of Vaporization	16.4 – 18.1 kJ/mol
11	Heat of Fusion	2.89 – 3.247 kJ/mol
12	Specific Heat Capacity	94 J/kg.K
13	Enthalpy of Fusion	2.7 kJ/mol
14	Enthalpy of Vaporization	18.1 kJ/mol
15	Thermal Entropy	176.1 kJ/mol.K (at 298.15
16	Thermal Conductivity	3.61 mW/m.K at 300 K
17	Electrical Conductivity	0.1 mOhm-cm
18	Polarizability	5.3 Å ³
19	Ionization Energy	10.745 eV
20	Density	0.00973 g/cm ³ at 293 K

1.6.1 Health effects of radon:

Radon is categorized as a human carcinogen (Group I) by the International Agency for Research on Cancer (IARC, 1988). The breakdown of radon into its progeny results in the generation of alpha radiations. Although the alpha particles released by radon and its progenies lack the energy to penetrate even the skin of a

human body, once swallowed or inhaled, they can easily interact with internal organs, particularly the lungs, and can alter the DNA structure, producing mutations and hence cancer.

Radon is constantly generated in soil and emitted into the atmosphere. Due to the progenies produced during the chain decay these radioactive gases are considered hazardous in spite of their short half-life. Atmospheric radon is not a health risk because it is swiftly diluted to low levels by circulations in outdoor air. When it is concentrated in enclosed areas such as buildings, caves, and mines, it creates a hazard to the environment. Therefore indoor air pollutant in houses, to which all human beings are exposed, can be considered as the main topic of health concern. The main sources of indoor radon (i.e. in an enclosed space) are soil gas emanation from soils and rocks, water and natural gas used, which later off-gas into indoor air, building materials, and directly from the outdoor atmospheric air through openings such as doors, windows, ventilations, and so on. The annual exposure to radon, thoron and their progenies contributes greatly to the annual effective dose. The concentration of radon in houses varies greatly due to ventilation of houses. In houses with poor ventilation, variations in atmospheric pressure can cause variations in radon concentration. (Stranden, E., Berteig, L., and Ugletveit, F., 1979). Although the majority of radon ingested is quickly expelled, a small amount can mix with other molecules in the air, dust particles, smoke, aerosols, and so on, depositing itself in the airways and lungs once inhaled. Radon progenies, due to their short half-life, release ionising alpha radiation when lodged, damage the sensitive cells in lung tissue, such as the basal cells of the bronchial epithelium (National Research Council, 1988). As a result, radon and its isotopes have previously been identified as the second leading cause of lung cancer after tobacco smoking (Hassan *et al.*, 2011; Mujahid *et al.*, 2010; WHO, 2009). The risk of lung cancer after exposure is substantially higher in cigarette smokers than in non-smokers who have never smoked (Darby *et al.*, 2005). According to WHO (2009), "Radon is far more likely to cause lung cancer in those who smoke or have smoked in the past than in lifelong non-smokers." It is, nevertheless, the leading cause of lung cancer in persons who have never smoked." The potential effects and nature of the harm induced will be determined by the level of exposure.

1.6.2. Radon in soil:

The presence of radon in the living environment can be attributed to both natural and manmade causes. Natural background radiation sources include emissions from the earth's crust's dirt, rocks, and ore bodies, as well as emissions from various building materials such as bricks, cement, tiles, and so on.

The concentration of radon in soil is influenced by soil moisture content, barometric pressure variations, temperature and structure of soil. The transportation of radon from the source to the environment (gas or liquid medium) is accomplished by

(a) Emanation - This is the process by which radon atoms produced by radium decay escape from the grains (mostly due to recoil) and enter the interstitial space between the grains. In this process, radon is released into small air or water contained in pores between soil and rock particles which is facilitated by diffusion and convection

(b) Transport - Diffusion and advective flow carry the emitted radon atoms via the soil matrix's pore space to the ground surface.

(c) Exhalation — radon atoms moved to the earth surface and subsequently released into the atmosphere. Radon and thoron are usually produced in soil as a result of the presence of ^{238}U and ^{232}Th containing minerals.

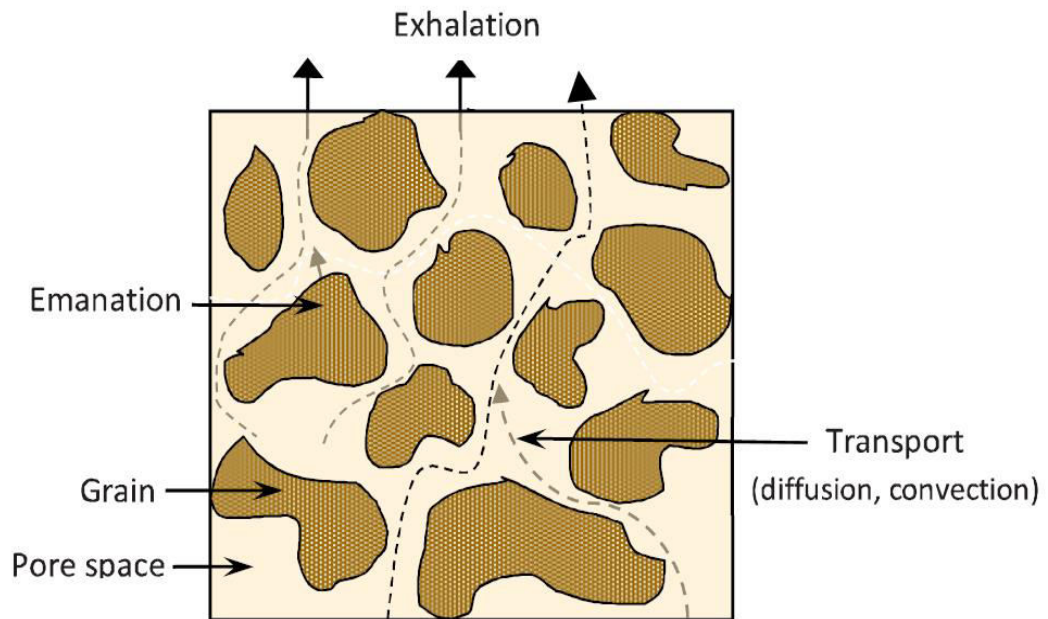


Figure 1.3: Movement of radon in soil

Radon or thoron is only free to travel in the earth's crust or other porous matrix if their atoms make their way into pores or capillaries. Although the specific processes responsible for radon emission from grains are not well known, it is assumed that recoil reactions contribute significantly to radon emanation. Temperature has a minor impact on radon emission, whereas moisture content has a significant impact. This is due to the fact that a radon atom entering a pore that is fully or partially filled with water has a higher possibility of being halted in the pore volume without crossing the pore space, and being exhaled out in the atmosphere can increase this probability. Radon is transported from the pore space to the environment mostly through diffusion and, in some situations, through darcian flow (Advection). There are numerous extrinsic factors that might affect diffusivity and thus exhalation rate. Rain, snow, ice, and increases in air pressure reduce exhalation rate, whereas increases in wind speed and temperature enhance it.

1.6.3 Measurement techniques:

There are numerous devices and procedures available for measuring radon, thoron, and their decay products. These approaches are based on the detection of

alpha, beta, or gamma ray radiations generated by them separately or in combination. The instruments employed are classified into three types based on their sample methods: grab (or instantaneous), integrating, and continuous. Instruments can be either active or passive.

(a) Scintillation cell grabbing method: The most common grab sampling method for measuring radon in air is sucking the gas through a filter paper into a scintillation flask or cell. A sample of air is drawn into a flask or cell that has a zinc sulphide phosphor coating on its inside surfaces and is sealed in this technique. One side of the cell has a clear window that is in contact with a photomultiplier tube to count light pulses (scintillations) caused by alpha disintegrations in the air sample reacting with the zinc sulphide covering. The number of pulses is related to the cell's radon concentration.

(b) Double filter method: Air is passed through a cylinder with a high efficiency filter at each end to trap the progeny in this approach. The cylinder volume ranges from 0.5 to 1000 l, and the typical sample time is 5 to 30 minutes. The inlet filter filters out the short-lived offspring from the tested air. The exit filter gathers the progeny generated inside the cylinder as it travels from one end to the other. Information on radon/thoron levels can be obtained by measuring the activity gathered on the exit filter.

(c) Continuous radon monitors: Three types of online monitors are widely used. The online radon monitor functions as an ionisation chamber in the first type. Radon in the ambient air diffuses into the chamber via a filtered region, causing the radon concentration in the chamber to follow the radon concentration in the ambient air with a slight time lag. Within the chamber, alpha particles released by radon atom decay cause bursts of ions that are recorded as distinct electrical pulses corresponding to each disintegration. The monitor electronics process these pulses, and the number of pulses counted is usually shown on the monitor. The most popular commercially available radon detector of this type is the AlphaGuard. The second type of online radon monitor is based on solid-state silicon detectors. It works by directing ambient air through a filter into a detecting chamber. As radon decays, the decay products are gathered via an electric field onto a solid-state silicon detector,

such as a PIN diode, where the alphas generated by the decay of these products are detected. RAD7 and RTM-2200 are common instruments of this type. The ambient air is sampled for radon in a scintillation cell after passing through a filter that filters radon decay products and dust in the third type of monitor. The radon decay products plate out on the internal surface of the scintillation cell as the radon in the cell decays. The scintillation cell and a photomultiplier detect alpha particles produced by future decays or the first radon decay.

1.7 Smart RnDuo:

The RnDuo is a highly advanced portable continuous radon/thoron monitor developed for a variety of radon and thoron research. Figure 1.4 depicts the schematic diagram of the microprocessor-based RnDuo. For radon measurements, sample gas is collected by diffusion into a scintillation cell (150 cc). During diffusive sampling, the gas is routed via a "progeny filter" and a "thoron discriminator," which removes radon/thoron progenies and thoron. The "diffusion-time delay" thoron discriminator does not allow the short-lived thoron ^{220}Rn (half-life 55.6 s) to pass through. RnDuo's radon measurements are based on the detection of alpha released by radon and its decay products within a scintillation cell volume. The PMT and the related counting electronics continually count the alpha scintillations produced by radon and its decay products inside the cell. The accumulation and degradation of radon decay products inside the scintillation cell as a result of fluctuating radon concentrations is complex, and they never achieve equilibrium with radon. As a result, automated continuous radon monitoring was not achievable without accounting for decay product activities. In-house, a fantastic algorithm was created for the effective implementation of scintillation technology to continually assess radon levels. The algorithm is based on the predicted decay and increase of radon decay products throughout the existing measurement cycle, as well as radon concentrations in the past.

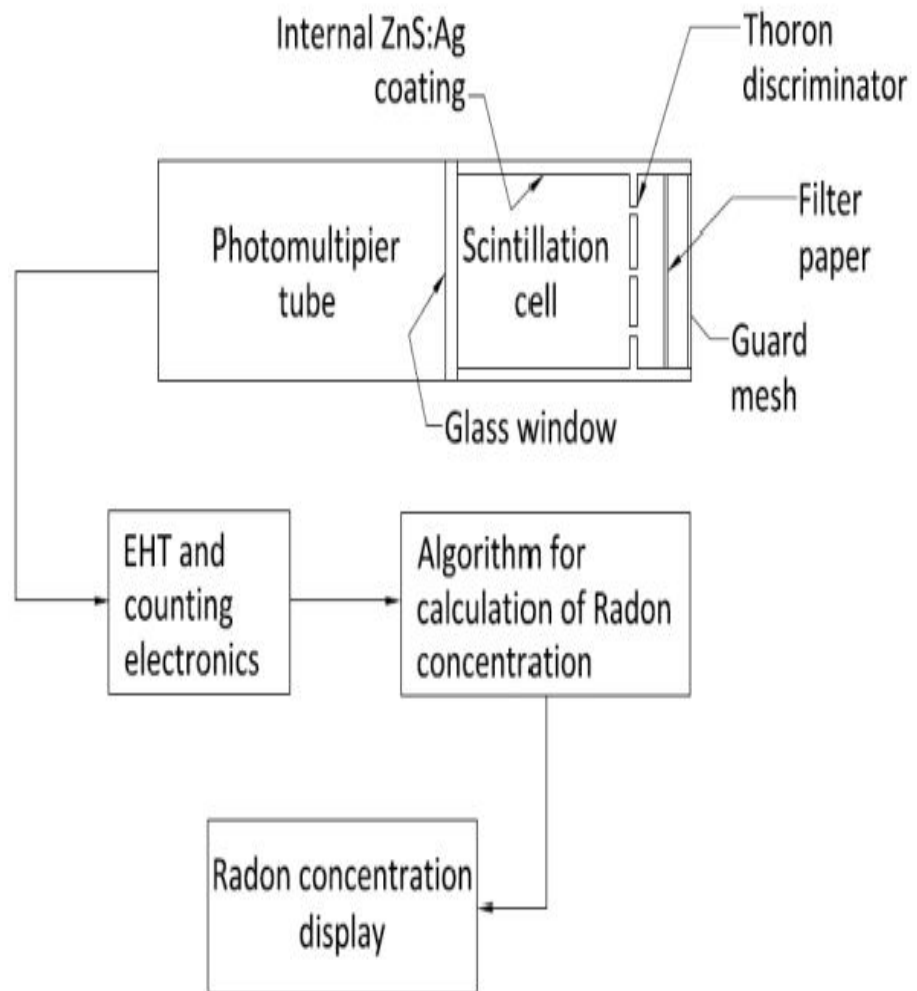


Figure 1.4: Schematic of radon measurement process in RnDuo

1.8 Faults:

A fault is a fracture or zone of fractures that exists between two rock blocks. They are fissures in the Earth's crust caused by rocks sliding past each other on either side of the crack. The fractures can be as thin as hair at times, with hardly perceptible movement between the rock layers. However, faults can be as short as a few millimetres or as long as thousands of kilometres. Faults enable the blocks to move in relation to one another. This movement can occur quickly, as in an earthquake, or slowly, as in creep. The majority of faults cause recurring displacements over geologic time. During an earthquake, the rock on one side of the fault abruptly shifts with regard to the rock on the other. The fault surface could be horizontal, vertical, or any angle in between. The movement of rocks in faults are associated with movement of radon in the soil. The concentration of radon in soil gas is determined by geology, soil porosity, structure (shears, faults, and thrusts), and the presence of uranium mining in the area. The geology of the area may also contribute to high indoor radon concentrations. (Choubey, V. M., Sharma, K. K., & Ramola, R. C., 1997)

The core of the Earth constantly emits heat, which is transmitted out through the layers, heating the asthenosphere closest to the centre of the Earth. When a rock gets heated, it tries to cool down. To accomplish this, it moves away from the centre and grows. This rock cools as it climbs toward the earth's surface, but there is additional rock beneath it that is heating up and rising as well. The newly heated rock requires the rock to move out of the way, so it moves out of the way and gradually sinks back closer to the centre of the Earth. Convection currents in the asthenosphere are caused by rock movement. The earth's outer layer is divided into tectonic plates. The plates move due to convection currents in the asthenosphere underneath them. This movement is responsible for the formation of geographical structures and events such as mountains, volcanoes, and earthquakes. The plate motion isn't a smooth, consistent motion. Because of friction between the plates, they move in quick jumps, which we call earthquakes.

The state of Mizoram is located on the north eastern part of India comprising of hilly areas and a tropical region with moderate climate. The Kurlok faults are located on the northern parts of Mizoram on Kolasib district area. The fault lines located at the different regions of the district are as shown in figure 1.5

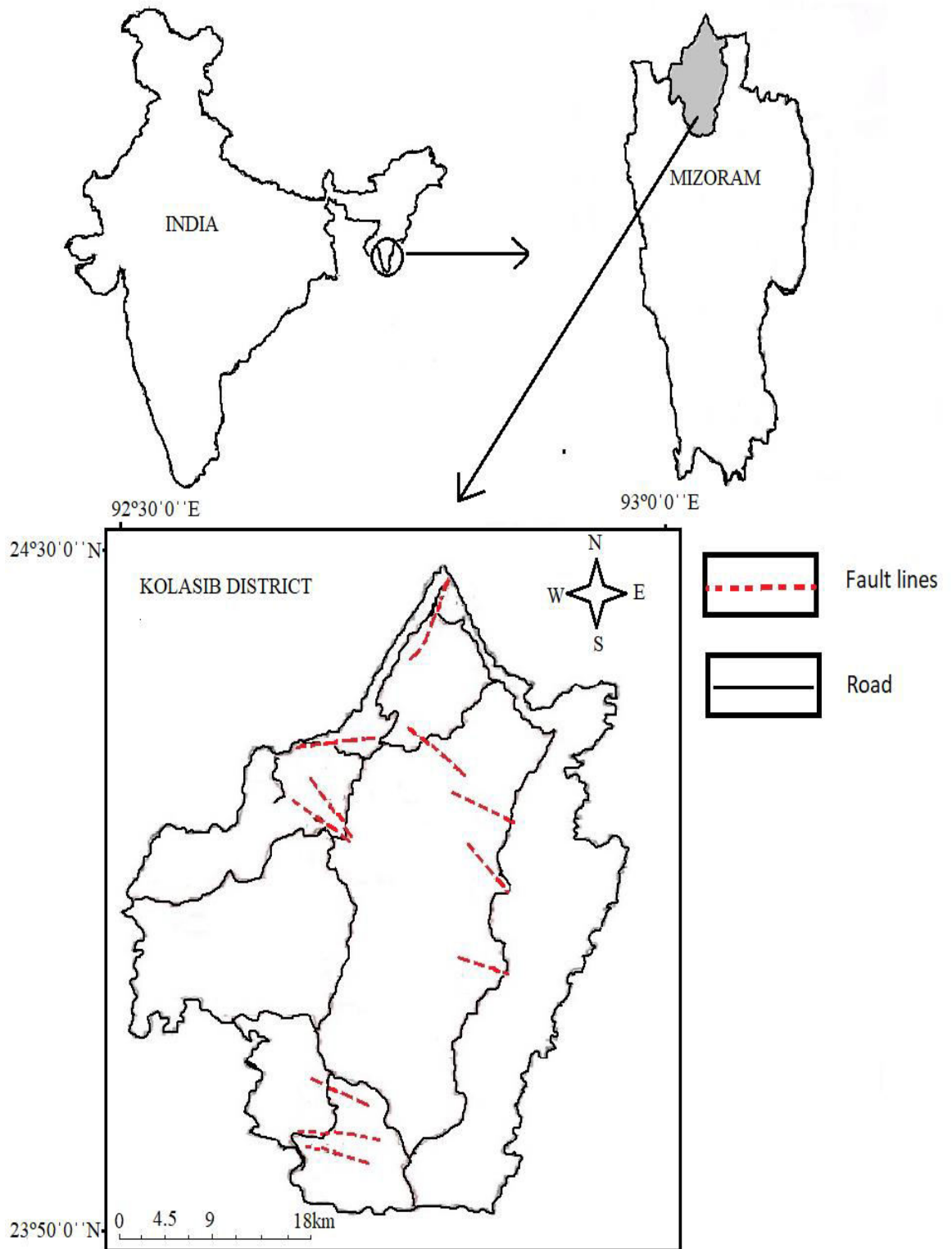


Figure 1.5: Geographical map of study area with fault lines

1.9 Review of literature:

Research regarding radon has been going on in different parts of the world for quite some time in the past. The concentration of natural radionuclide in air, soil, and water has been studied in several places of the world. Initially, investigations were conducted primarily with the goal of correlating to epidemiological studies, identifying radioactive materials found in soil and rocks, and predicting earthquakes. All of these investigations have resulted in the advancement of measuring and detection tools, as well as improvements in theoretical formulation and experimental processes to produce more precise results. The carcinogenic character of natural radionuclides such as radon was discovered during a study of uranium miners conducted by Jacobi (1993), Nagaratnam (1994), and others around the world. Passive methods like LR – 115 nuclear track detectors have been in use for measuring Rn-222 and U-238 contents in soil samples in various regions of Sudan giving an average value of radon exhalation rate from the soil. (Hafez A.F. *et al.* 1991). Radon flux measurements have also been measured using direct techniques like static chamber in Malaga Spain. It was found that the factors that most affected the Rn-222 release were the humidity and soil thermal gradient. (Duenas *et al.* 1996). In Garhwal Himalayas radon exhalation rate was measured using emanometry technique. The results was found that the soil-gas radon concentration and radon exhalation rate are somewhat higher than the normal value and depend on the lithological formation of the area (Ramola, R., and Choubey, V., 2003)

Soil characters have been studied as well. Compared with soil radium contents, radon exhalation rate from soil and soil radon concentrations are more easily impacted by soil characters and change in a rather large range (Sun, K., Guo, Q., and Cheng, J., 2004).

Short term temporal variations of soil gas radon were studied using different measurement techniques using Lucas cells, continuous monitor integral nuclear track-etch detectors. It was seen that a low variability appeared during a 72h follow up. Different temporal changes were observed by using different methods. A substantial part of these changes was caused by fluctuations and errors connected with measuring methods themselves and did not reflect real variations of the

measured parameter (Nezmal *et al.* 2004). Radon exhalation rate from collected soil samples have been measured in South Kumuan Lesser Himalayas using LR-115 Type II plastic track detector. The correlation coefficient between radium contents in collected soil samples and soil-gas radon from the same locations was calculated as 0.1, while it is 0.2 between radon exhalation rate and soil-gas radon concentration. The results show weak positive correlation due to the geological disturbance in the equilibrium conditions and high mobility of radon in the same geological medium (Prasad *et al.* 2008)

In other parts of India Solid State Nuclear Track Detectors (SSNTD) have been used for measuring exhalation rate of soil samples in Noonmati, Guwahati Assam in which a good correlation was observed between radium content and radon exhalation rate in soil samples (Sarma H.K. *et al.*, 2011). Other places of India such as Uttar Pradesh, radium content and radon exhalation rates were studied in using LR-115 track detectors. All the values of radium content in soil samples of study area were found to be quite lower than the permissible value of 370 Bq kg⁻¹ recommended by Organization for Economic Cooperation and Development. (Verma, D., Khan, M. S., and Zubair, M., 2012)

Recently radium and radon exhalation rates in soil samples were studied in areas of Northern Rajasthan using LR 115 type – II plastic track detectors. It was found that mass exhalation samples vary from 8.27 to 23.19 m Bq kg⁻¹h⁻¹ with average of 14.96 m Bq kg⁻¹h⁻¹ and surface exhalation of 273.80 – 768.04 m Bq m⁻² h⁻¹ with average of 495.32 m Bq m⁻² h⁻¹. Radium concentration from 6.88 – 19.31 Bq kg⁻¹ with average of 12.45 Bq kg⁻¹. Hence the area is considered safe for health and does not pose any environmental health hazard (Duggal, V., Mehra, R., and Rani, A., 2015). Study of exhalation rate in soil samples were also studied in other parts of Kathmandu valley using passive detector LR 115. It was found that higher value of radon exhalation rate was found in the soil samples corresponding to dwellings with high indoor radon concentration (Parajuli, P., Thapa, D., and Shah, B. R., 2015).

Srivastava *et al.* (1996) conducted measurements of potential alpha energy of radon and its progenies in several regions of Aizawl, Kolasib, Saiha, and Khawlian in 1996, which was one of the early investigations on natural radionuclide measurement in Mizoram. Almost a decade later, the concentrations of radon,

thoron, and their progeny were measured in 17 Mizoram homes (Ramachandran *et al.*, 2003). Rohmingliana *et al.*, (2009) and Vanchhawng *et al.* (2009) measured radon and thoron concentrations in the Mizoram districts of Aizawl, Champhai, and Kolasib in 2009. In Mizoram, soil gas radon and thoron concentration measurements have been carried out in Mat Fault using LR-115 type II detectors. The measurements were carried out in a 15 day interval and was found that the data obtained have been correlated with the seismic activities that occurred around the measuring site. Positive correlations were found between radon/thoron data and the earthquakes (Jaishi *et al.* 2014, 2015,). Continuous measurements of radon concentration at 80 cm inside the soil were also carried out at Chite Fault (23.73°N, 92.73°E), Aizawl, Mizoram situated in the seismic zone V in North Eastern part of India near Indo-Burma subduction zone, using LR-115 Type-II nuclear track detectors. Certain anomalies observed in radon concentration have been correlated to the earthquakes within the range of magnitudes $4.7 \leq M \leq 5.5$, while some other anomalies are due to the influence of meteorological parameters. (Singh *et al.*, 2016). Radon and thoron concentrations were measured in the districts of Aizawl, Kolasib, and Champhai using solid-state nuclear track detectors to provide time integrated concentration values of indoor radon and thoron. Champhai District had the greatest radon/thoron concentrations of the three districts, while Kolasib District had the highest thoron concentration (Rohmingliana *et al.*, 2010). Radon concentrations in houses were also measured in Mamit Districts for almost two years, from May 2009 to February 2011. Meteorological studies regarding to ^{222}Rn and ^{220}Rn have also been carried out along with pre seismic thoron anomaly (Thuamthansanga *et al.*, 2021). Most of the work done here are all studies regarding to soil, but many studies have also been done by researchers in regards to radon in water. But since this study is mainly based on soil, radon in water will not be mentioned here. This is the first time the areas of Kurlok fault regions along with faults of Kolasib district are being studied.

The objectives of this present study includes:

- Soil gas emanation study along Kurlok fault regions of Kolasib district
- To generate a gamma dose rate map of the study regions.
- Modeling of exhalation rate along the fault regions.

The study of soil gas is carried by Smart RnDuo device with in-situ measurements along the fault regions selected for this study. The results from this study will be significant for determining the concentration of radon in soil gas along the fault regions. Spot gamma radiation measurement and soil radioactivity measurement will help in determining the gamma dose rate and provide necessary data for radiological exposure to the general population. Gamma survey meter and NaI detectors will be used for this process. As for exhalation rate, Smart Rnduo device will be used to measure soil samples extracted from the selected fault regions.

THEORY AND METHODOLOGY

In this chapter, we will go through the theoretical formulation as well as the many methodologies used in the current study work. This chapter will also provide a full description of the detectors or devices that were employed. Scintillation based detector Smart RnDuo was used for measuring radon mass exhalation from soil samples and for measuring radon concentration in soil gas with the help of a soil probe. Spot background gamma radiation was measured using survey meter PM 1045 at each sampling site at a height of 1m above the ground. The soil were collected from the sampling sites and the activity concentration of uranium, potassium and thorium were measured using a gamma spectrometer, Sodium Iodide, NaI (TI) Detector, coupled with a personal computer based 1K multi-channel analyzer, GSPEC-SA. The soils collected from the sites were measured using a mechanical sieve shaker to determine the grain size distribution. In this present work, study was conducted on the fault regions Kurlok fault regions as well as the other fault regions of Kolasib District, Mizoram.

The sampling areas lie within Kolasib District area of Mizoram with the fault lines and smpling areas given as shown in figure 2.1. The areas extend from 92° 30' 0'' E to 93° 0' 0'' E longitude and 24° 30' 0'' N to 23° 50' 0'' N latitude. For each selected fault line, three areas area selected in which soil samples are collected to be measured for mass exhalation, soil type determination and activity concentration measurement. As for radon concentration in soil gas, in-situ measurement is carried out on each site at different depths.

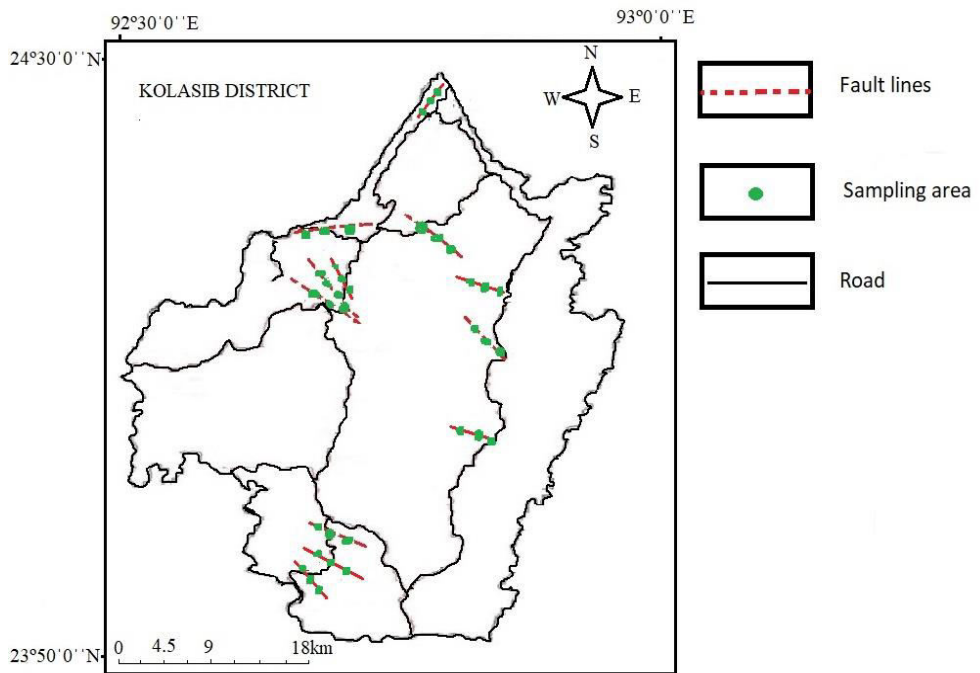


Figure 2.1: Sampling areas of Kolasib District

2.1: Smart RnDuo

Smart RnDuo, a scintillation-based radon detector, is a portable, advanced continuous radon/thoron detector developed by Bhabha Atomic Research Centre in Mumbai, India, with numerous applications in radon and thoron studies (Figure 2.2). The sample gas was collected into a scintillation cell (150 cc) by diffusion for radon concentration determination. The gas was passed through a "progeny filter" and a "thoron discriminator," which removed the concentrations of radon/thoron progenies and thoron. Because the thoron discriminator is based on "diffusion-time delay," the short-lived thoron ^{220}Rn , with a half-life of only 55.6 seconds, is not allowed to pass through.

The Smart RnDuo's radon concentration measurement is based on the detection of alpha particles released by radon and its decay products, which form inside a scintillation cell volume. The Photo Multiplier Tube and the related counting electronics continuously count the alpha scintillations produced by radon and its decay products manufactured inside the cell.

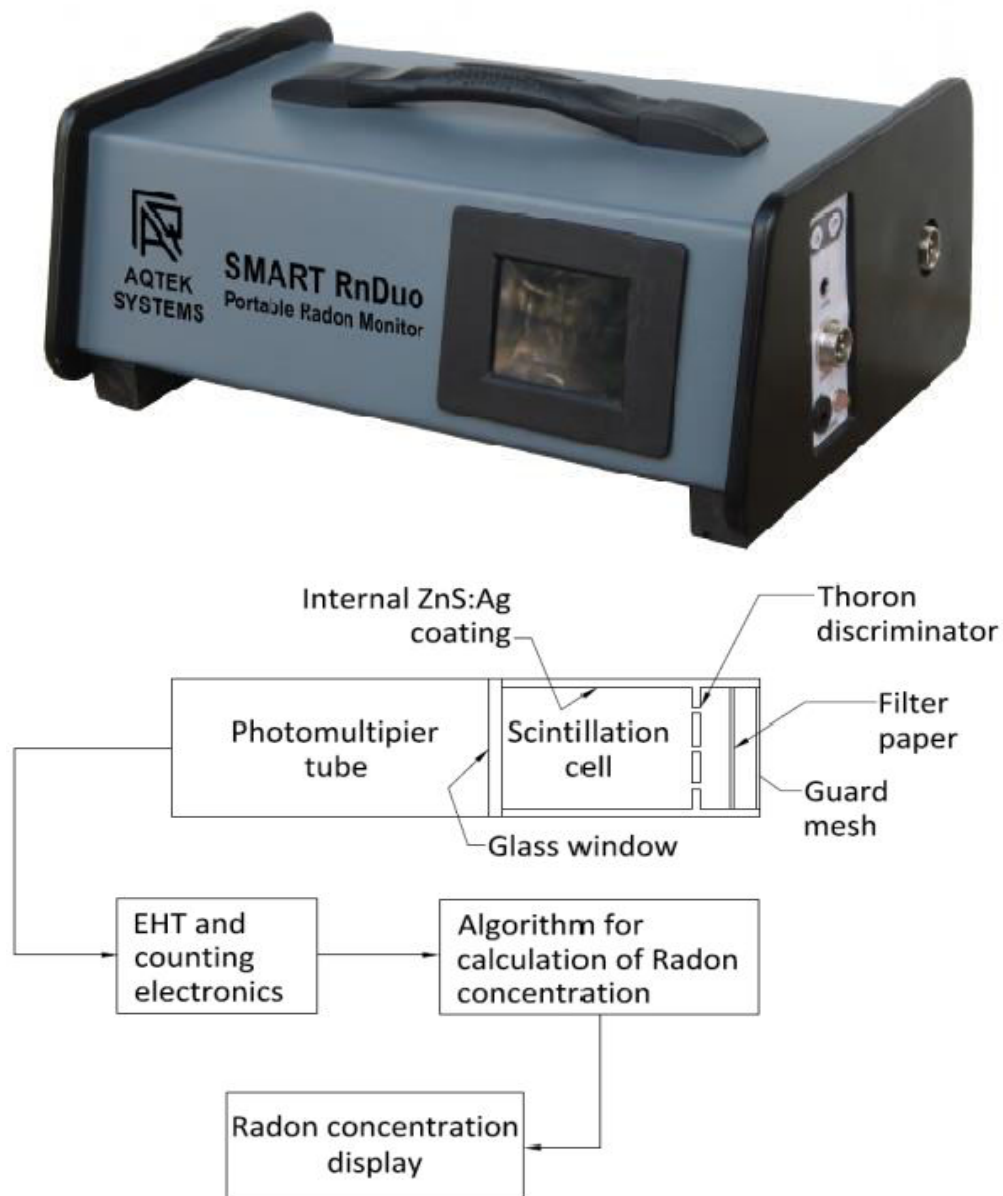


Figure 2.2: Schematic diagram of Smart RnDuo

The accumulation and decay of radon progenies inside the scintillation cell as a result of fluctuating radon concentrations is complex, and they never reach equilibrium with radon. As a result, automated continuous radon monitoring was not achievable without accounting for decay product activities. To address this shortcoming, an in-built algorithm for the successful deployment of scintillation technology to continuously measure radon concentration was developed.

The above-mentioned in-built algorithm is based on the theoretical decay and increase of radon decay products during the existing measurement cycle, as well as the radon concentration in the past. The alpha counts recorded when measuring radon concentration are processed by a microprocessor unit according to the developed algorithm, and the actual radon concentration is presented on the monitor. The instrument has a high sensitivity and a small detector volume, making it an excellent choice for radon detection. Smart RnDuo was utilised in this study to evaluate the radon concentration in soil gas as well as the radon mass exhalation rate in soil due to its good features and portability.

Table 2.1: Technical specifications of Smart RnDuo

Detector type	Scintillation cell	
Scintillation coating	Internally coated ZnS:Ag	
Scintillation cell active volume	153 cm ³	
Radon sensitivity	1.2 CPH/(Bq/m ³)	44.5 CPH/ (pCi/L)
Thoron sensitivity	0.8 CPH/(Bq/m ³)	30 CPH/ (pCi/L)
Sampling type	Diffusion / Flow	
Sampling flow rate	0.5to0.7L/minwithinbuilt pump	
Measurement cycle time	15 / 30 / 60 min	
Response time	15 minutes for attaining 95% of radon / thoron	
Minimum detection limit	Radon: 8 Bq/m ³ at 1 σ and 1 h cycle Thoron: 15 Bq/m ³ at 1 σ and 1 h cycle	

Upper detection limit	50 MBq/m ³
Effect of sample humidity and trace gases on sensitivity	Practically nil until humidity is not condensed on scintillator surface.
Thoron interference	< 5% with sniffing mode of sampling
Power	External: 110-240VAC 50/60Hz Internal: 6 V DC Battery
Dimension	37 cm x 20 cm x 12 cm

2.1.1: Smart RnDuo for measurement of radon mass exhalation rate from soil

The radon mass exhalation rate governs the radon emission potential from soil (Jm). The radon mass exhalation rate has been routinely measured using both active and passive methods. Although both methods of measurement produce accurate and comparable results, active methods are found to be more advantageous for exhalation studies because they require much less time for measurement, typically 1-2 days, whereas passive methods, typically using a solid state nuclear track detector, take about 3 months at a time. The radon mass exhalation rate of obtained soil samples was assessed using an active technique in this study, using a Smart RnDuo monitor combined with a radon mass exhalation chamber donated by BARC, Mumbai.



Figure 2.3: Measurement of Radon Mass Exhalation Rate using Smart RnDuo

The accumulation chamber is a stainless steel cylinder with an interior height of approximately 8 cm and a radius of approximately 4.5 cm. To produce a closed loop measuring method, the scintillation detector was mounted directly to the upper or top side of the accumulation chamber, acting as a lid. The closed loop measurement technique aids in the accumulation of radon concentrations within the chamber and enables precise radon mass exhalation measurement.



Figure 2.4: Mass exhalation chamber

The measurement is based on the detection of α -particles released by radon gas from soil samples, as well as their decay progeny created inside the detector chamber by scintillation using ZnS. (Ag). RnDuo has a response time of about 20 minutes for 63 percent of chamber radon concentration and 40 minutes for 95 percent chamber radon concentration.

Soil samples were carefully collected at each sampling site by first removing the top or upper part of the dirt (up to a few centimetres) and then collecting the resulting soil in a plastic/polythene bag. The soil samples were collected in such a way that for each fault line on the area, three samples were collected by means of gardening tools. The acquired sample was weighed and its volume was taken before being placed into the radon mass exhalation chamber to measure the rate of radon mass exhalation. The scintillation detector was then put on top of the exhale chamber, and radon build up data was received every 60 minutes for a period of 10 to 24 hours. The protocol for operation of RnDuo for mass exhalation measurement is shown in Appendix – I. The acquired data was fitted using least squares using the equation given below (Sahoo *et al.*, 2007; Lekshmi *et al.*, 2018)

$$C(t) = \left(\frac{J_m M}{V} \right) t + C_o \text{ ----- (2.1)}$$

Where C (t) is ^{222}Rn concentration (Bq m^{-3}) at time t, C_o is the ^{222}Rn concentration (Bq m^{-3}) present in the chamber volume at $t = 0$, M is the total mass of

the dry sample (Kg) and V is the effective volume (volume of detector + porous volume of sample + residual air volume of mass exhalation chamber) (m³).

The porous volume (V_p) can be estimated using the following equation:

$$V_p = V_s - \left(\frac{M}{\rho_g} \right) \text{-----} (2.2)$$

Where V_s is the sample volume in the mass exhalation chamber. ρ_g is the specific gravity of the sample which can be taken as 2.77 gm/cc for clay type soil material. t is the measurement time (h).

Upon least square fitting of the data to the above equation one may obtain J_m from the fitted parameters with the information of the mass M of the sample.

Because of the presence of its parent radionuclide, radium, radon gas is continually generated in the soil matrix. After formation, it emanates from the soil matrix into the surrounding air or water pockets enclosed between the pores between rocks or soils. The radon emission factor is defined as the fraction of radon atoms that depart the solid phase in which they are created and become free to travel through the bulk media. The formula for calculating the emanation factor (f) is: (Lekshmi *et al.*, 2018)

$$f = \frac{J_m}{C_{Ra} \lambda} \text{-----} (2.3)$$

Where,

C_{Ra} is the radium activity concentration (Bq/kg),

λ is the decay constant of radon (in hour),

J_m is the mass exhalation rate of radon (mBq/kg/hr).

2.1.2: Modeling of exhalation rate with measured and calculated values:

The exhalation rates obtained are compared with calculated values with a method provided by UNSCEAR 2000. The effective diffusion coefficient, porosity, ²²⁶Ra concentration, soil density, and the emanation coefficient can all be used to calculate the radon exhalation rate. We used this connection to determine radon exhalation rate and compared the findings to the measured exhalation rate. The radon exhalation rate J was

determined using the radium-in-soil concentration A_{Ra} .

$$J = \sqrt{D_e \cdot \lambda} \cdot f \cdot \rho \cdot (1 - \varepsilon) \cdot A_{Ra} \text{ ----- (2.4)}$$

Where f is the soil emanation coefficient of radon, ρ is the soil particle density ($\text{kg} \cdot \text{m}^{-3}$), and D_e is the effective diffusion coefficient of radon ($\text{m}^2 \cdot \text{s}^{-1}$) obtained from Rogers and Neilson (1991).

2.1.3: Measurement of Radon in soil gas using soil probe:

Radon gas concentrations are monitored on the ground at depths of 60 cm, 90 cm, and 120 cm along the Kurlok fault zones using a scintillation-based detector Smart RnDuo. The Smart Rnduo is built in such a way that it will have a minimum interference from humidity. A soil probe of appropriate length is placed into the ground and connected to the Smart RnDuo device through pipes attached at various ends. For each location, measurements are obtained every 15 minutes for nearly an hour, totaling 4 to 5 readings. The average of the obtained readings is computed. For comparison, measurements are collected at different depths of 60 cm, 90 cm, and 120 cm along the Kurlok fault zones as well as the other fault regions of the Kolasib District. The protocol for deployment and operation of RnDuo for measurement of Radon concentration in soil gas is shown in Appendix – II

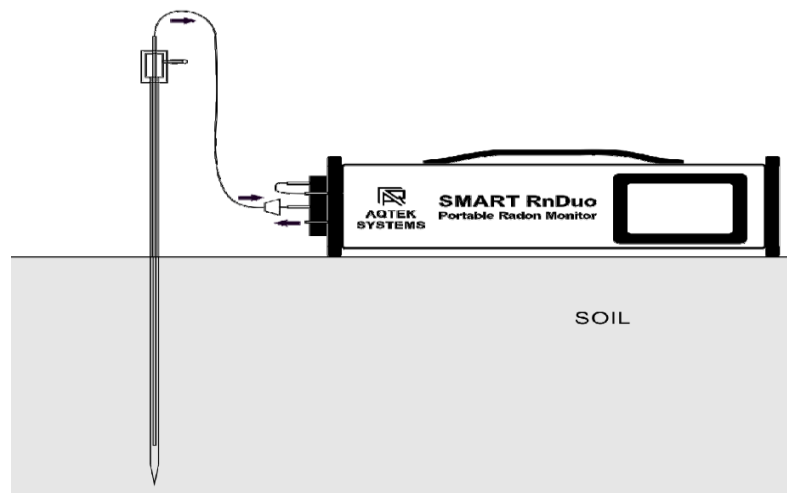


Figure 2.5: Measurement of Radon concentration in soil gas using Smart RnDuo

2.2: Gamma Spectrometry using NaI(Tl) Detector

For measurement of soil radioactivity, NaI (TI) based gamma-ray

spectrometric technique was used. This method is nondestructive and does not necessitate any chemical separation of radionuclides. In addition, the activity of many radionuclides in a single sample can be determined simultaneously. This technique, while simple, rapid, and sensitive, has one drawback: it necessitates a somewhat higher sample size. It is determined by the gamma emission of several radionuclides in the ^{232}Th and ^{238}U radioactive decay chain. Although all of these two series' daughter products are radioactive, not all of them generate powerful gamma rays. Based on the energy of the emission, each gamma emission can be easily identified. Gamma emissions from a few daughter products in these chains, namely ^{228}Ac , ^{212}Pb , ^{212}Bi , and ^{208}Tl in the ^{232}Th series and ^{214}Bi and ^{214}Pb in the ^{238}U series, can be used to not only identify radionuclides but also estimate their activity.

The samples were kept sealed for one month to determine the establishment of secular equilibrium between ^{226}Ra and ^{228}Th and their corresponding daughter products. This is because the gaseous daughter products of the ^{232}Th and ^{238}U series, ^{220}Rn and ^{222}Rn , decay to particulate radionuclides with half-lives of 55 seconds and 3.8 days, respectively. If the container is not airtight, the gaseous daughters will be lost, and the readings will be incorrect. As a result, the sample containers are kept sealed so that no ^{220}Rn or ^{222}Rn spills out. In secular equilibrium, the parent's half-life is substantially longer than the daughter's half-life, and the secular equilibrium is reached after seven half-lives of a daughter.

Calibration standard sources can be in any matrix for energy calibration, but for efficiency, calibration standard sources must be in a similar matrix and geometry since the density of the sample matrix and its geometry impacts the attenuation factor for gamma rays. To reduce the inaccuracy in activity estimation, standard sources with similar geometries and known concentrations were also produced.

The correct identification of photopeaks in the spectrum produced by the detector system and the assessment of its activity are required for the estimation of gamma emitting radionuclides in the sample. While energy calibration creates an accurate relationship between channel number and gamma energy, efficiency

calibration identifies the exact activity of a radionuclide, i.e. the standard used in efficiency calibration. A gamma-ray spectroscopy system's energy calibration is a relationship between the energy deposited in the detector by a gamma ray and the amplitude of the matching amplifier output pulse. The Multi-Channel Analyzer is used to calculate pulse amplitude in terms of channel number. The energy calibration is also utilised to identify the photopeak resolution and the location of regions of interest (ROIs).

Thallium (Tl) activated 5”x 4” Sodium Iodide (NaI) detector was connected to a PC based multi-channel analyzer also known as GSPEC-SA (Version 2.5 X) which was manufactured by Electronic Enterprises (India) Pvt. Ltd, Mumbai, Maharashtra, India (Figure 2.7). The GSPEC-SA allows control and analysis of the detector output by employing in-built computer-based application software (SAAS – Spectrum Acquisition and Analysis). GSPEC-SA is a 1K Multichannel Analyzer with HV Supply and Spectroscopy Amplifier.

Gain	HV	LLD	¹³⁷ Cs Ch & Energy		⁶⁰ Co Ch & Energy		⁶⁰ Co Ch & Energy	
			Channel	keV	Channel	keV	Channel	keV
6	650	1	231	661.99	403	1173	455	1332.01

Figure 2.6: Initial settings of multi-channel analyzer

The detector is encased in a cylindrical lead and iron shield to counteract the effects of background radiation from the surrounding environment. The Multi-Channel Analyzer has been pre-calibrated to detect gamma energies ranging from 0 to 3000 keV. For this aim, two standard sources were used: ¹³⁷Cs, with an energy peak at 661.99 keV, and ⁶⁰Co, with two energy peaks at 1173 keV and 1332 keV.



Figure 2.7: NaI Detector connected with GSPEC-SA

2.2.1: Efficiency and Energy Calibration of NaI(Tl) Detector

For efficiency calibration, an IAEA standard source of ^{238}U , ^{232}Th , and ^{40}K (Figure 2.8) with known activity was evaluated for 10800 seconds using the GSPEC-SA multichannel analyzer (3 hours). This calibration determined the detector's detection efficiency as a function of radiation energy. To reduce inaccuracy due to gamma radiation attenuation, all three standard sources were designed with same geometry and matrices. In addition, to avoid gamma ray coincidence summing, a gamma ray standard of the same radionuclide as the one to

be monitored was utilized (Agarwal, 2011)

The gamma ray photons emitted by the radioactive decay chain of the standard sources interact with the detector in a variety of ways, resulting in a complicated detector response with a continuous energy distribution and definite complete energy peaks. This continuous energy distribution is caused by some of the photon energy being absorbed inside the detector volume, while the remainder of the photon energy escaping from the detector. The full energy peaks are caused by the total absorption of gamma photons within the detector, which can be caused by the photoelectric effect or by a variety of simultaneous interactions. The efficiency was determined using the formula for the obtained gamma energy peak:

$$\eta(\%) = \frac{\text{Area/Sec}}{\text{dps}} \times \frac{100}{\text{Ab}\%} \times 100 \text{-----} (2.5)$$

Where,

$\eta(\%)$ = Percent Efficiency

Area/Sec= Net peak area per second (background subtracted)

dps = Source strength

Ab% = Gamma ray abundance factor

Before detecting the natural radioactivity in a sample, a three-point energy calibration was performed with sources containing a radionuclide combination (ISO 18589-3:2007(E)). The energy calibration in this work is accomplished by counting specified standard sources of ^{60}Co and ^{137}Cs for 500 seconds. This calibration enables the construction of a relationship between the analyzer's channel numbers and the known energy of photons (BIPM, 2004). After analysing the region of interests (ROIs), the appropriate calibration was accomplished by inputting the collected data into the computer software. The protocol for efficiency and energy calibration is shown in Appendix III and IV.



Figure 2.8: IAEA Standard Sources for Energy and Efficiency Calibration

2.2.2: Activity Concentration Measurement

The collected samples were first dried before being heated with a heater to around 110 °C. The samples were then ground into a fine powder and sieved through a 500 N mesh sieve. It was then put inside a 250 ml airtight container and left undisturbed for at least 30 days to achieve radioactive equilibrium. The sample's activity concentration was determined by studying it for 50,000 seconds with the GSPEC-SA Multichannel Analyzer. After reducing the background radiation content, the activity concentrations for three primordial radionuclides, ^{238}U , ^{232}Th , and ^{40}K , were calculated using the multichannel analyzer programme. The activity concentration was determined solely for ^{238}U , ^{232}Th , and ^{40}K radionuclides in this study because these are the most prominent and plentiful natural radionuclides found in nature. As previously stated, the activity concentrations of ^{238}U and ^{232}Th in soil samples cannot be detected directly using gamma spectroscopy. However, because secular equilibrium has been established between ^{238}U , ^{232}Th , and their decay products, the ^{238}U concentration was calculated using the activity concentrations of its daughter radionuclide, ^{214}Pb , and the ^{232}Th concentration was calculated using the activity concentrations of its decay radionuclide, ^{228}Ac . The ^{238}U -series (^{214}Pb), ^{232}Th -series (^{228}Ac), and ^{40}K activity concentrations are all expressed in Bq/kg. Following measurement, the weights of the samples were measured, and the activity concentration (A) for each sample was calculated using the formula below:

$$A = \frac{N}{T} \times \frac{100}{\gamma\%} \times \frac{100}{\eta\%} \times \frac{1}{Wt} \text{-----} (2.6)$$

Where,

N/T = Background subtracted net photo peak counts in time 'T'.

γ = abundance of gamma ray under consideration.

η = absolute detection efficiency obtained from the energy efficiency calibration.

Wt = weight of the sample

2.2.3: Determination of Radium Equivalent Activity And Hazard Indices:

The uniformity of natural radioactivity in soil in relation to radiation exposure is characterised in terms of the Radium equivalent activity (Raeq). It compares the specific activity of materials with varying quantities of ^{226}Ra , ^{232}Th , and ^{40}K . Since radioactive equilibrium was attained for all soil samples, the activity level of ^{238}U obtained in this study matches to the activity level of its daughter radionuclide, ^{226}Ra .

Radium equivalent activity (Raeq) is essentially a single statistic that represents the activity levels of ^{226}Ra , ^{232}Th , and ^{40}K while accounting for the radiation dangers associated with them. It is defined as follows, assuming that 370 Bq/kg for ^{226}Ra , 259 Bq/kg for ^{232}Th , and 4810 Bq/kg for ^{40}K generate the same gamma dose rate (Beretka *et al.*, 1985):

$$Ra_{eq} (\text{Bq/kg}) = C_U + 1.43 C_{Th} + 0.077 C_K \text{-----} (2.7)$$

Where,

C_{Ra} represents the activity concentrations of ^{226}Ra (in Bq/kg)

C_{Th} is the activity concentrations of ^{232}Th (in Bq/kg)

C_{K} is the activity concentrations of ^{40}K (in Bq/kg)

The external hazard index assesses the risk of natural gamma radiation and this index is used to determine a material's radiological compatibility. The primary goal of this index is to keep the radiation exposure below the permissible dose equivalent limit of 1 mSv y^{-1} . Internal exposure to radon and its compounds is assessed in addition to the exterior danger index by estimating the internal hazard index.

Inhaling alpha particles from the short-lived radionuclides radon and thoron is similarly harmful to the respiratory organs. The formula for External and Internal hazard indices are given by (Quindos *et al.* 1987)

$$H_{ex} = \frac{C_U}{370} + \frac{C_{Th}}{259} + \frac{C_K}{4810} \text{----- (2.8)}$$

$$H_{in} = \frac{C_U}{185} + \frac{C_{Th}}{259} + \frac{C_K}{4810} \text{----- (2.9)}$$

2.5: Spot background gamma detection

Background gamma radiation will be detected using the Gamma Survey Meter PM 1405 and a Geiger-Muller counter via photon-to-electro-pulse conversion. The equipment was created by Polimaster, a Russian business that specializes in radiation measuring and detection systems. The Survey Meter measures the amount of beta radiation flux emitted from polluted areas of gamma and X-ray equivalent ambient exposure levels. When the preset radiation levels are achieved, the instrument alerts the operator with an auditory warning and records each detected count in a search mode with an audio signal.

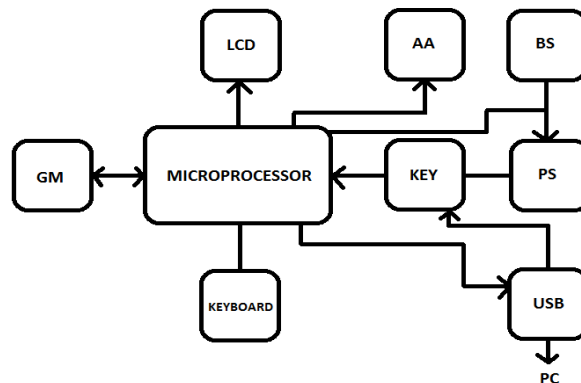


Figure 2.9: Gamma Survey Meter PM 1405

Through opening the special screen-filter and selecting beta-radiation flux density measurement mode, the instrument enables to estimate the surface exposure level of different environmental objects from beta radiation sources. The instrument is compact in size and has a lightweight, large LCD backlight display, audible warning, and non-volatile memory.

Technical Specifications:

Detector: Geiger-Muller counters

Dose equivalent rate (DER) measurement range: 0.1 $\mu\text{Sv/h}$ – 100 mSv/h

DER indication range: 0.01 $\mu\text{Sv/h}$ – 130 mSv/h

DER measurement accuracy: $\pm (20 + K/H) \%$, where \dot{H} – dose rate, $\mu\text{Sv/h}$ K - coefficient 1.0 $\mu\text{Sv/h}$

Dose equivalent (DE) measurement range: 1.00 μSv – 10.0 Sv

DER indication range: 0.01 μSv – 10.0 Sv

DE measurement accuracy: $\pm 20 \%$

PC communication: USB interface

Measurements will be taken at 1 metre above ground level to detect background gamma radiations from cosmic and terrestrial sources. The instrument's operation algorithm enables measuring process continuity, static processing of measurement findings, rapid adaptability to variations in radiation rate, and effective output of information obtained on the LCD. The measurement range for gamma radiations varies from 0.1 Sv h^{-1} to 100 mSv h^{-1} . The protocol for operation of Gamma survey meter Pm1405 is shown in Appendix –V. The Global Positioning System (GPS) device will be used to determine the latitudinal and longitudinal coordinates of sampling sites.

2.6: Soil type and grain size determination:

The textural soil classification system of the United States Department of Agriculture (USDA) was used to classify soil types. Sand, silt, and clay are the three fundamental soil classifications (Garcia-Gaines *et al.*, 2015). The rate of radon mass exhalation is discovered to be highly controlled by soil moisture content. The grain size of different types of soil varies, and the grain size impacts the soil's ability to hold moisture. As a result, identifying soil type and determining grain size is critical in this regard.

A sieve shaker is a tool used to determine the kind of soil and grain size. It is made up of a sieve stack, which is made up of sieves of varying mesh sizes placed on top of one another. The sieve with the largest mesh holes is on top, followed by a sieve with a tighter mesh size than the one above it. When the Sieve Shaker is agitated, soil of various grain sizes settles in the various stages. Soil type and grain size can be determined in this manner. Soil analysis is an important technique because it may provide a wealth of information about soil and how it will respond under various uses, stressors, and climates.

To identify the grain size distribution, five different sieve mesh numbers were used: 60 (grain size 0.25 mm, which corresponds to medium sand), 120 (grain size 0.125 mm, which corresponds to fine sand), 230 (grain size 0.0625 mm, which corresponds to very fine sand), 325 (grain size 0.044 mm, which corresponds to silt/mud), and >325 (grain size smaller than 0.044 mm. The soil that had

accumulated on each sieve was then removed and the weight was calculated. The derived percentage of the grain size distribution was then shown using a triangle plot. The triangle plot is divided into three fundamental classifications: sand, silt, and clay. These three categories are further subdivided into 12 classes. For this objective, a triangular layout known as the USDA triangle was used (Garca-Gaines *et al.*, 2015). The various grain sizes obtained in this investigation were named using the Udden-Wentworth size term (Wentworth, 1922).



Figure 2.10: Mechanical Sieve Shaker

Determination of Radon Mass Exhalation Rate, Radon Concentration in Soil Gas and Soil Grain Size Distribution

The determination of radon mass exhalation, radon in soil gas and the type of soil grain size distribution are presented in this chapter. This section will contain the details of the results and a few discussions on each topic. The results obtained will be compared with results from different locations. For mass exhalation areas of Kurlok consisting of different fault regions around the areas of Kolasib district will be taken into consideration as well as some areas of Aizawl district for comparison purposes. For soil gas, Kurlok fault regions are compared with the surrounding areas of Kolasib district and also determine its variation with depth of soil. The grain size distribution will make use of the samples obtained from the mass exhalation process of areas of Kolasib district.

3.1: Measurement of radon mass exhalation rate:

The study area is located at north-east of India on Kolasib district in the state of Mizoram which lies in the seismic zone V of seismic zonation map of India. The geographical sites where the soil samples were collected from the fault lines are as shown in figure 3.1. Kolasib district is located on the north of Aizawl which is the capital of the state Mizoram. It is a tropical region with moderate climate. The sampling area extends from N 23° 53' 29.57" to N 24° 28' 16.1" latitude and E 092° 39' 33.97" to E 092° 47' 41.09" longitude.

As illustrated in figure 3.1, soil samples were obtained from 36 different places within the research area. Soil samples were gathered in such a way that three samples were collected for each fault line in the area using gardening equipment. Depending on the structure of the soil, the soil is burrowed a few centimeters deep, and the topmost layer is avoided when sampling the soil. The samples are then returned to the lab to be measured and analysed.

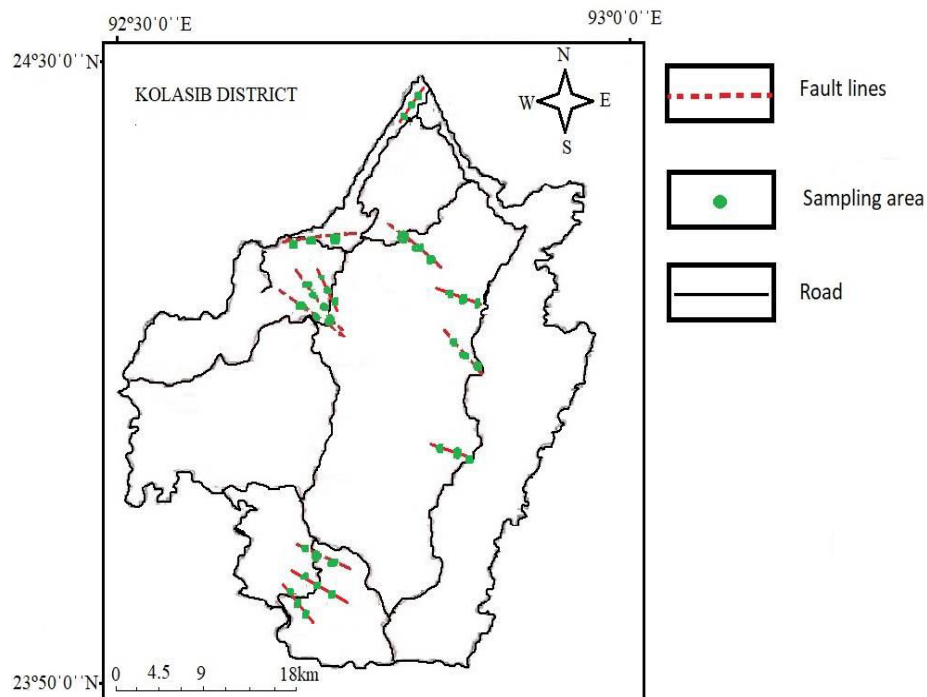


Figure 3.1: Geological map of the study area for mass exhalation

3.1.2 Results and Discussion:

The results of the mass exhalation from soil samples collected from different fault lines are shown in table 3.1. The exhalation rates varies as seen from the data with minimum value of $2.3 \text{ mBqkg}^{-1} \text{ hr}^{-1}$ at K25 and maximum value of $45.7 \text{ mBqkg}^{-1} \text{ hr}^{-1}$ at K23 and K31. The mass exhalation rates ranges from $2.3 \text{ mBqkg}^{-1} \text{ hr}^{-1}$ – $45.7 \text{ mBqkg}^{-1} \text{ hr}^{-1}$ with an average of $20.42 \text{ mBqkg}^{-1} \text{ hr}^{-1}$. The variation in exhalation may be due to rainfall and moisture content in the soil as soil moisture content plays a significant role in exhalation (M. Faheema and Matiullah, 2008). The results obtained from this are comparable to work done in Northern Rajasthan with an average value of 14.96 mBq/kg/hr (V. Duggal *et al.*, 2015), Kangra District, Himachal Pradesh with an average value of 19.91 mBq/kg/hr (D.K. Sharma *et al.*, 2003) and Kathmandu Valley, Nepal with an average value of 6.4 mBq/kg/hr (P. Parajuli *et al.* 2015). We can see that there are different variations in different places when compared with each other. This may be due to the fact that these areas are located at very far away from each other and hence different locations have

considerable differences in geology of the areas of study. The differences in structure of the land and soils play an important part in exhalation process. The presences of uranium in rocks underneath the earth are also the cause of high radon exhalation.

Table 3.1: Measurement of radon mass exhalation from fault regions of Kolasib district

Location code	GPS Coordinate	Radon mass exhalation rate (mBq/kg/h)	Location code	GPS Coordinate	Radon mass exhalation rate (mBq/kg/h)
K1	Elevation 23 m N 24° 20' 45.23" E 092° 40'08.88"	8.2	K19	Elevation 48 m N 24° 20' 58.1" E 092° 45'32.0"	9.9
K2	Elevation 36 m N 24° 20' 51.39" E 092° 40'17.69"	11.9	K20	Elevation 38 m N 24° 20' 57.5" E 092° 45'23.5"	11.5
K3	Elevation 44 m N 24° 20' 58.15" E 092° 40'32.85"	24.6	K21	Elevation 37m N 24° 20' 59.0" E 092° 45'16.6"	6.5
K4	Elevation 260 m N 24° 15' 27.80" E 092° 40'36.50"	35.5	K22	Elevation 49 m N 24° 28' 11.5" E 092° 46'54.9"	45.3
K5	Elevation 351 m N 24° 15' 11.15" E 092° 40'37.48"	25.4	K23	Elevation 53 m N 24° 28' 16.1" E 092° 46'53.4"	45.7
K6	Elevation 431 m N 24° 14' 49.92" E 092° 40'56.08"	35.9	K24	Elevation 58 m N 24° 28' 15.7" E 092° 46'56.6"	26.2
K7	Elevation 385 m N 24° 14' 52.80" E 092° 41'36.26"	45.0	K25	Elevation 350m N 24° 14' 56.4" E 092° 41'12.3"	2.3
K8	Elevation 410 m N 24° 14' 59.27" E 092° 41'34.60"	12.8	K26	Elevation 360m N 24° 14' 55.2" E 092° 41'12.6"	9.8
K9	Elevation 403 m N 24° 14' 41.37"	10.0	K27	Elevation 49 m N 24° 28' 11.5"	9.9

	E 092° 41'24.56"			E 092° 46'54.9"	
K10	Elevation 474 m N 23° 53' 29.57" E 092° 40'23.97"	11.0	K28	Elevation 53 m N 24° 28' 16.1" E 092° 46'53.4"	11.5
K11	Elevation 468 m N 23° 53' 39.61" E 092° 40'25.25"	7.6	K29	Elevation 58 m N 24° 28' 15.7" E 092° 46'56.6"	6.5
K12	Elevation 447 m N 23° 54' 14.22" E 092° 40'26.09"	5.6	K30	Elevation 350m N 24° 14' 56.4" E 092° 41'12.3"	45.3
K13	Elevation 186 m N 23° 55' 59.81" E 092° 40'19.32"	27.7	K31	Elevation 360m N 24° 14' 55.2" E 092° 41'12.6"	45.7
K14	Elevation 138 m N 23° 56' 04.76" E 092° 39'46.88"	28.4	K32	Elevation 365m N 24° 14' 52.3" E 092° 41'11.8"	26.2
K15	Elevation 152 m N 23° 56' 00.50" E 092° 39'33.97"	6.7	K33	Elevation 679m N 24° 14'12.85" E092°48'26.37"	2.3
K16	Elevation 271 m N 23° 57' 59.14" E 092° 40'54.97"	28.8	K34	Elevation 695m N 24° 13'55.04" E092°48'24.42"	9.8
K17	Elevation 313 m N 23° 57' 19.59" E 092° 41'04.06"	35.7	K35	Elevation 683m N 24° 13'44.86" E092°48'17.95"	21.6
K18	Elevation 311 m N 23° 57' 11.55" E 092°41'06.12"	32.7	K36	Elevation 582m N 24° 12'06.28" E092°48'30.34"	18.95

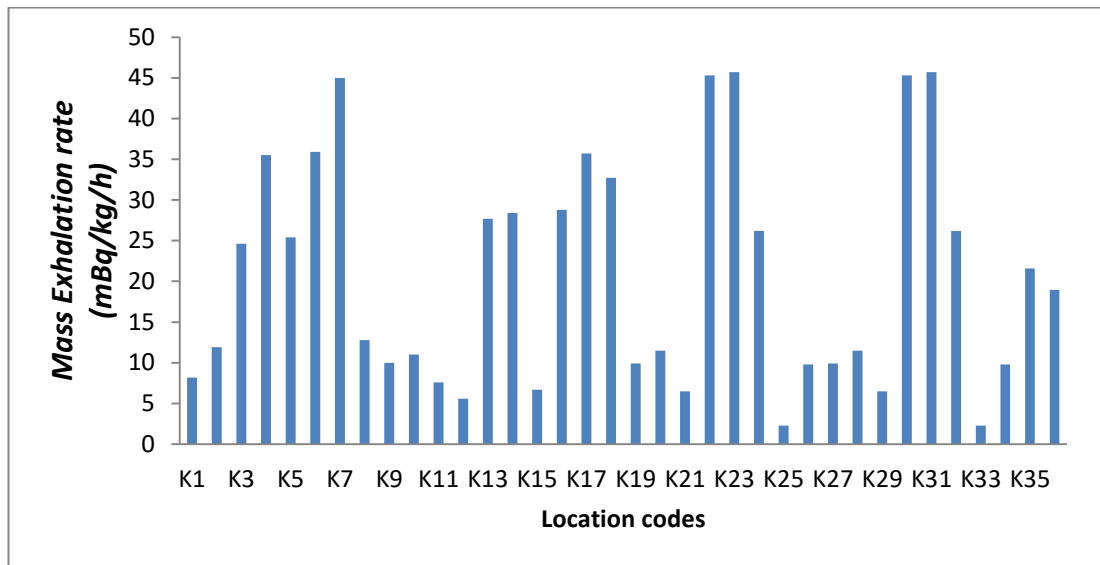


Figure 3.2: Radon mass exhalation from fault regions of Kolasib District.

3.1.1: Modeling of radon exhalation:

For modeling purpose, the measured and calculated values of exhalation rates have been compared as shown in table 3.2 . The calculated values lies within the range of 4.21 mBq/kg/hr to 31 mBq/kg/hr with an average value of 18.7 mBq/kg/hr and standard deviation of 9.44 mBq/kg/hr. The comaprison results shows few significant differences between the measured and calculated values.The ratio of calculated and measured values ranges from 0.39 to 3.86 with an average of 1.07. From the results we can see that at some locations the measured values area higher and in some loactions the calculated values are higher due to soil moisture content having different variations with different locations. As mention before soil moiture content plays an important role in exhalation as well as geology of the areas. Aside from this parameters such as porosity, temperature and humidity also affects exhalation rates. In some cases artificial structure like piplines within the soil can also affect the path of radon within the soil (Hosada *et al.*, 2009). The method of comparison would be more suitable if the measurements were taken in a more controlled environment. Figure 3.3 and 3.4 shows the distribution of measured and calculated values of exhlalation rates from the falut regions of Kolasib district.

Table 3.2: Comparison table of measured and calculated exhalation rates.

Location	Calculated value (mBq/kg/hr)	Measured value (mBq/kg/hr)	Ratio
K1	5.95	14.9	0.39
K2	15.08	20.9	0.72
K3	31.17	8.06	3.86
K4	27.	32.4	0.83
K5	21.96	22.6	0.97
K6	27.27	32.2	0.84
K7	12.55	14.2	0.88
K8	9.54	16.3	0.58
K9	29.95	23.2	1.29
K10	16.2	11.23	1.44
K11	24.49	39.1	0.62
K12	4.21	9.3	0.45

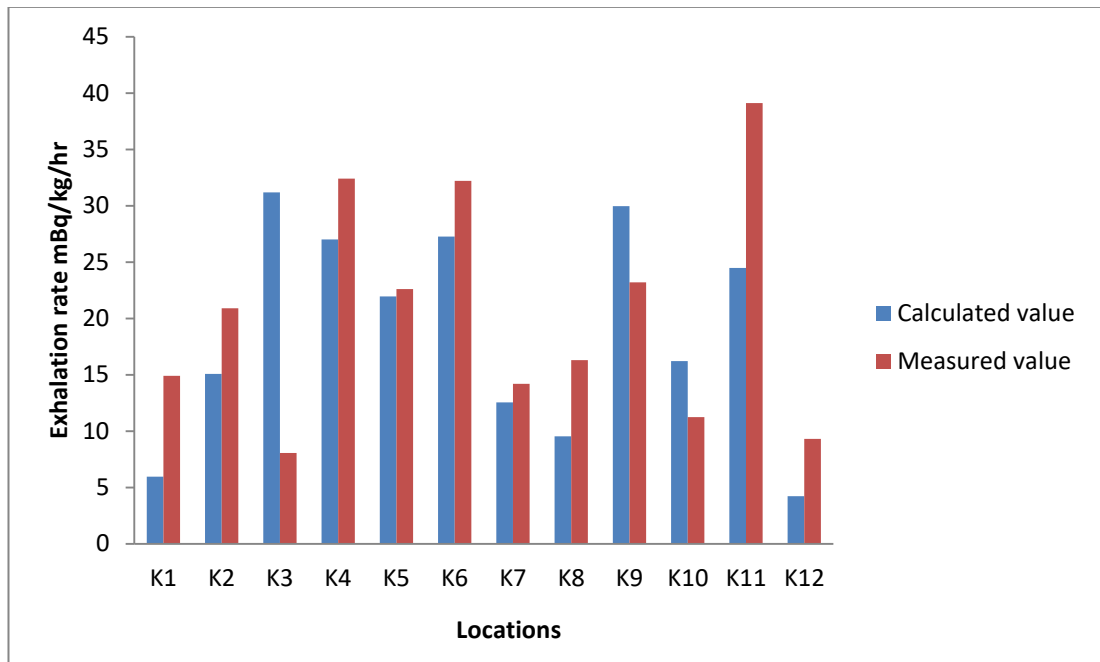


Figure 3.3: Comparison figure of measured and calculated exhalation rates.

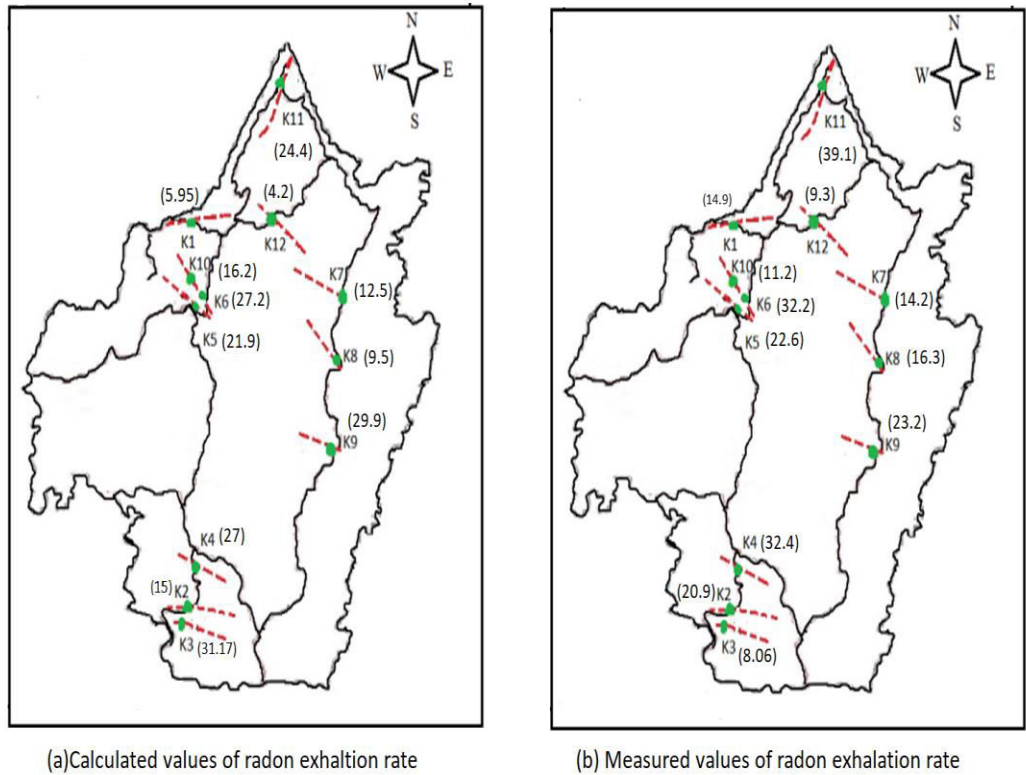


Figure 3.4: Geographical map of measured and calculated exhalation rate.

Apart from this, measurements have been taken in some fault regions of Aizawl District for comparison analysis. The sampling area extends from $23^{\circ}22'39.5''$ to $24^{\circ}09'30.16''$ latitude and $92^{\circ}39'49.03''$ to $92^{\circ}56'49.35''$ longitude. Soil samples were collected from 33 different fault locations within the study area. The values of radon exhalation in soil samples from fault regions ranges between 11.2 mBq/kg/hr - 72.2 mBq/kg/hr with an average of 39.92 mBq/kg/hr and standard deviation of 13.5 mBq/kg/hr . We can see that there are differences in average exhalation rates and this may be due to the differences in geology of different areas.

Table 3.3: Measurement of radon mass exhalation from fault regions of Aizawl district

<i>Location code</i>	<i>GPS Coordinate</i>	<i>Radon mass exhalation rate (mBq/kg/h)</i>	<i>Location code</i>	<i>GPS Coordinate</i>	<i>Radon mass exhalation rate (mBq/kg/h)</i>
A1	Elevation 1161 m N 23° 24' 23.8" E 092° 45' 07.0"	27.9	A18	Elevation 511 m N 23° 09' 30.16" E 092° 56' 49.35"	30.6
A2	Elevation 1151 m N 23° 24' 29.1" E 092° 45' 06.3"	29.2	A19	Elevation 147m N 23° 51' 06.94" E 092° 49' 57.61"	11.2
A3	Elevation 1136 m N 23° 24' 29.6" E 092° 45' 13.1"	38.1	A20	Elevation 126m N 23° 50' 57.72" E 092° 49' 46.40"	30.2
A4	Elevation 155 m N 23° 43' 07.77" E 092° 48' 01.20"	35.1	A21	Elevation 147m N 23° 50' 43.61" E 092° 49' 53.89"	43.5
A5	Elevation 180 m N 23° 43' 18.16" E 092° 47' 51.70"	45.9	A22	Elevation 903 m N 23° 55' 56.67" E 092° 55' 47.21"	38.4
A6	Elevation 205 m N 23° 43' 22.72" E 092° 47' 50.37"	33.5	A23	Elevation 937 m N 23° 55' 51.84" E 092° 55' 38.28"	46.7
A7	Elevation 780 m N 24° 07' 19.09" E 092° 55' 07.96"	72.2	A24	Elevation 964 m N 23° 55' 45.77" E 092° 55' 37.88"	39.7
A8	Elevation 816 m N 24° 06' 22.95" E 092° 55' 16.11"	59.7	A25	Elevation 2647 ft N 23° 36' 18.4" E 092° 43' 19.5"	35.4
A9	Elevation 802 m N 24° 05' 57.51" E 092° 55' 00.03"	33.6	A26	Elevation 2728 ft N 23° 36' 16.5" E 092° 55' 38.28"	39.6
A10	Elevation 1178 m N 23° 28' 01.3" E 092° 43' 06.8"	51.2	A27	Elevation 2783 ft N 23° 36' 16.5" E 092° 43' 28.6"	21.3

A11	Elevation 1144 m N 23° 28' 04.4" E 092° 42' 52.4"	48.2	A28	Elevation 1012 m N 23° 39' 50.48" E 092° 49' 57.61"	44.2
A12	Elevation 1094 m N 23° 28' 23.0" E 092° 42' 46.9"	46.9	A29	Elevation 1014 m N 23° 39' 29.60" E 092° 40' 16.15"	69.4
A13	Elevation 1259 m N 23° 22' 46.7" E 092°45' 11.3"	34.2	A30	Elevation 861 m N 23° 39' 10.73" E 092° 40' 22.49"	53.6
A14	Elevation : 4212 ft N :23° 22'47.2" E 092° 45' 06.2"	15.5	A31	Elevation 872 m N 23° 39' 31.61" E 092° 42' 25.02"	46.8
A15	Elevation : 4104ft N : 23° 22' 39.5" E 092° 45' 14.8"	44.7	A32	Elevation 890 m N 23° 39' 36.73" E 092° 42' 28.65"	28.7
A16	Elevation 531 m N 24° 09' 04.37" E 092° 55' 53.07"	46.4	A33	Elevation 894 m N 23° 39' 40.88" E 092° 42' 37.18"	44.3
A17	Elevation 512 m N 24° 09' 18.14" E 092° 56' 42.09"	31.7			

3.2: Measurement of radon concentration in soil gas:

The goal of this research is to determine the distribution of radon concentrations in soil gas along the Kurlok Fault. This is the first study of radon concentrations in soil gas in the area. Radon gas concentrations are monitored on the ground at depths of 60 cm, 90 cm, and 120 cm along the Kurlok fault zones using a scintillation-based detector Smart RnDuo device. Other fault regions in Kolasib District were also measured at varying depths of 60 cm, 90 cm, and 120 cm for comparison purposes.

Kolasib's study regions are located in northern Mizoram, sharing borders with Assam. Kurlok fault zones are located on Rengtekawn junctions and are also known as Rengtekawn fault. The study region is located between 24° 11' 08.93" and

24° 20' 58.15" latitude and 92° 40' 32.85" to 92° 48' 34.25" longitude, with elevations ranging from 36 m to 568 m above sea level. Kurlok fault consists of a few kilometres of fault lines and covers the most area of the faults in Kolasib district. The area is crucial because, in theory, radon migration is supposed to be more prevalent around the places because they are considered to have more than one fault line. Radon concentrations in soil gas were detected using a scintillation-based detector, the Smart RnDuo, in various fault zones. The RnDuo is made up of a scintillation cell that is coated on the inside with ZnS:Ag. A photomultiplier tube is linked to this. The detection of alpha from radon and its decay products inside the scintillation cell is the basis for radon measurements. The photomultiplier tube and the related counting electronics count this. The outcomes are then displayed on the screen.

3.2.1 Results and Discussion:

Table 3.4 displays the results of radon concentrations in soil gas as well as the coordinates of each sampling site. The average radon concentrations in soil gas were 5.93 kBq/m³ at 120 cm depth, 2.93 kBq/m³ at 90 cm depth, and 0.13 kBq/m³ at 60 cm depth at the Kurlok Fault zones represented by K1, K2, and K3. The average radon concentration in soil gas in the other regions (K4-K7), on the other hand, was 3.77 kBq/m³ at 120 cm depth, 1.9 kBq/m³ at 90cm depth, and 0.12 kBq/m³ at 60 cm deep. We can see that the average concentration of soil gas is higher in the Kurlok fault zones than in the other districts. This could be because the Kurlok fault comprises of a larger or longer fault line that passes through the intersections. Because the passage of radon through rocks beneath the ground is dependent on faults, it is expected to be more concentrated in places with greater faults.

Table 3.4: Radon concentration in soil gas at different depths

Location code	Name of the location	GPS Coodinates	Concentration(kBq/m ³)		
			120 cm depth	90cm depth	60 cm depth
K1	Kurlok 1	Elevation 351 m N 24° 15' 11.15" E 092° 40' 37.48"	5.36	2.66	0.12
K2	Kurlok 2	Elevation 410 m N 24° 14' 59.27" E 092° 41' 34.60"	9.37	4.62	0.18
K3.	Kurlok 3	Elevation 552 m N 24° 14' 55.2" E 092° 41' 12.6"	3.06	1.51	0.11
K4.	Chemphai	Elevation 38 m N 24° 20' 57.5" E 092° 45' 23.5"	0.83	0.48	0.11
K5.	Buhchangphai	Elevation 36 m N 24° 20' 58.15" E 092° 40' 32.85"	6.29	3.09	0.15
K6.	Thingthelh	Elevation 587 m N 24° 11' 08.93" E 092° 48' 34.25"	6.13	3.13	0.13
K7.	New Khamrang	Elevation 313m N 23° 57' 19.59" E 092° 41' 04.06"	1.84	0.91	0.1

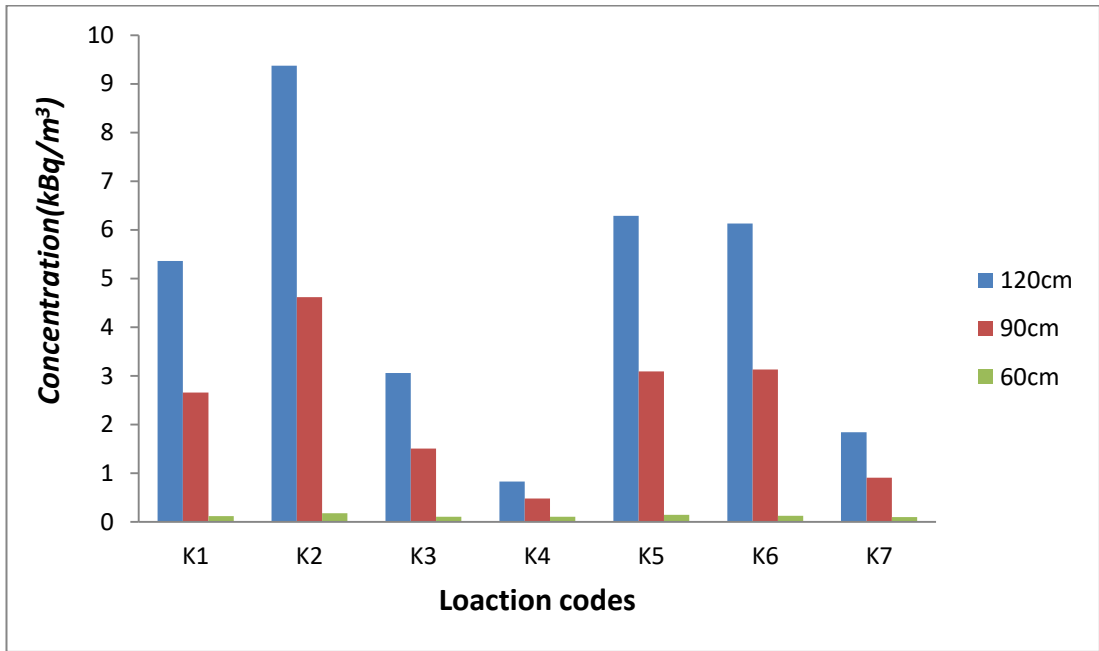


Figure 3.5: Radon concentration in soil gas at different depths

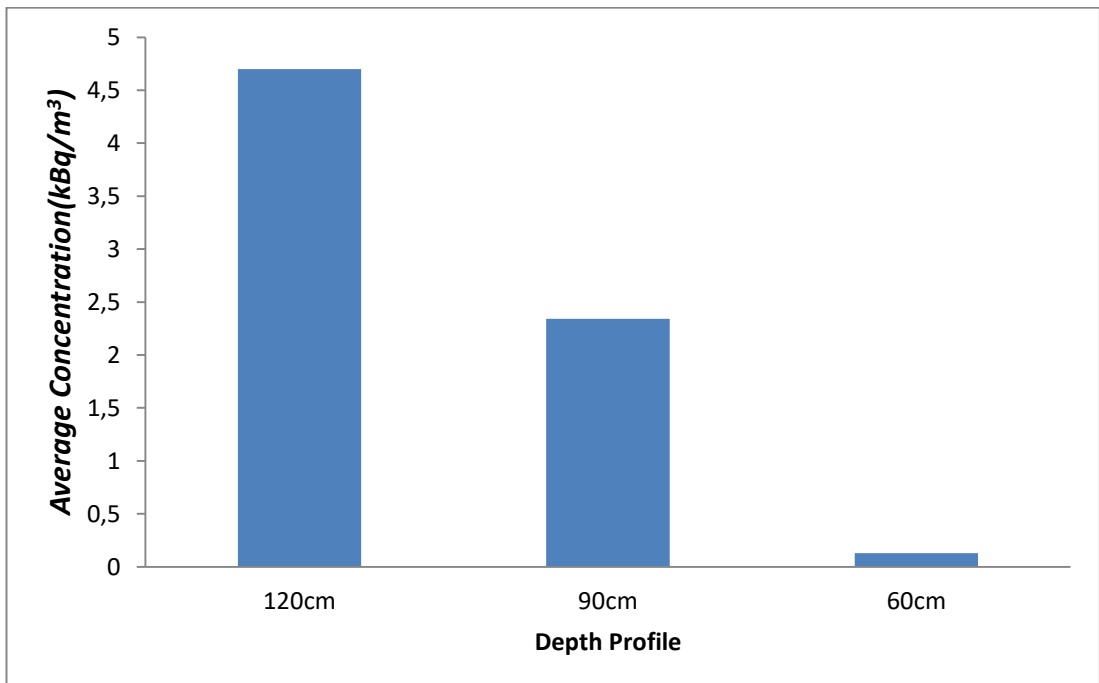


Figure 3.6: Average radon concentration in soil gas at different depths

The measured values of radon concentration from all the different locations lies between the range of 0.83 kBq/m³ to 9.37 kBq/m³ with an average value of 4.70 kBq/m³ at 120cm depth; from 0.48 kBq/m³ to 4.62 kBq/m³ with an average value of 2.34 kBq/m³ for 90cm depth and from 0.1 kBq/m³ to 0.18 kBq/m³ with an average value of 0.13 kBq/m³ for 60cm depth. The highest value of radon concentration for all the different depths lies in K2 having a value 9.37 kBq/m³ at 120cm, 4.70 kBq/m³ at 90cm and 0.18 kBq/m³ at 60cm depth while the lowest value for 120cm and 90cm lies in K4 with values of 0.83 kBq/m³ and 0.48 kBq/m³ respectively. The lowest value for 60 cm is on K7 with values of 0.1 kBq/m³.

The average concentration is higher at depths of 120cm than at other depths, according to the findings. On 60cm depth, the average concentration is the lowest. The findings show that the value of radon concentrations fluctuates depending on depth. The value of radon concentrations was found to increase when depth was increased. The difference in concentration could be related to changes in soil moisture content as the depth of the soil increases.

The results from this present investigation is compared with results from recent work done by other investigators and is shown in table 3.5. The results from this investigation is well within the ranges of results from South Kumaun Lesser Himalayas with concentration values of 1.10–31.80kBq/m³(Prasad *et al.*2008), Garhwal Himalaya with concentration values of 0.01–2.33kBq/m³ (Bourai *et al.*2013) and northern Rajasthan with concentration values of 0.09-10.40 kBq/m³(Vikas Duggal *et al.*2014). The differences in variation of concentration may be due to differences in geology of the different areas of investigations. The type of soil in different regions may be different and also the soil moisture content may vary depending on the location.

Table 3.5: Comparison of radon concentration of this present study with other investigators

Investigators	Radon concentration range (kBq/m ³)	Year	Area of investigation
Prasad <i>et al.</i>	1.10–31.80	2008	Budhakedar, TehriGarhwal, India
Bouraiet <i>al.</i>	0.01–2.33	2013	Garhwal Himalaya, India
VikasDuggalet <i>al.</i>	0.09–10.40	2014	Sri Ganganagar district, Rajasthan, India
Present investigator	0.1 – 9.37	-	Kurlok fault regions, Kolasib District, Mizoram, India

3.3: Soil Type Determination

Soil grain size analysis of soil samples was carried out using a mechanical sieve shaker, as the soil's ability to receive water is heavily influenced by the soil type and grain size distribution. And, because the moisture content of the soil may be responsible for the variation in radon mass exhalation, the soil type and grain size must be determined. The soil samples were fed through the Sieving Machine, and the soil was graded based on the amount of grain into sand, silt, or clay.

3.3.1 Results and Discussion:

Table 3.6: Determination of soil grain size from fault regions of Kolasib District:

Loaction codes	Percentage of		
	SAND	SILT	CLAY
K1	96.47	2.38	0.69
K2	95.90	2.99	1.04
K3	96.87	2.21	0.47
K4	97.74	1.77	0.46
K5	94.53	3.17	2.22
K6	95.36	3.46	0.94
K7	94.35	3.63	0.75
K8	98.60	1.04	0.03
K9	99.25	0.05	0
K10	98.45	1.04	0
K11	98.64	0.90	0.22
K12	97.63	1.34	0.62

Table 3.6 shows the grain size distribution from soil samples collected from fault regions of Kolasib District as well as the average values. It can be seen that a very high percentage of grain size was discovered to fall dominantly under "Sand," followed by "Silt," and then a very small percentage of grain size falls under "Clay" in all of the measured collected samples. The results obtained are then plotted using a triangular plotting proposed by USDA (United States Department of Agriculture). This is done with the help of computer software "Origin" to identify the soil type of the collected samples (Garcia *et al.*, 2015).

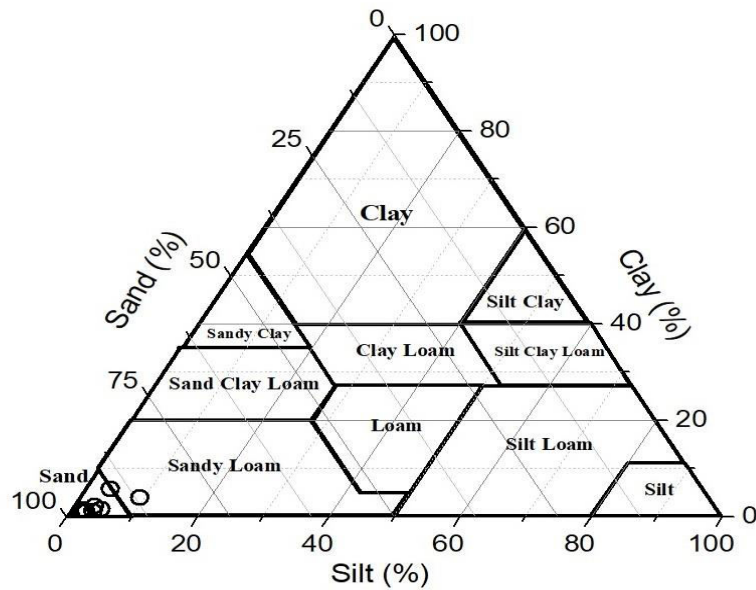


Figure 3.7: USDA triangular plot for soil samples from Kolasib District

Figure 3.7 depicts the USDA textural soil classification triangular plot. The results of the soil samples show that the majority of the soil particle size is distributed to a sandy kind of soil which is located at the left corner of the figure. Typically, the concentration decreases with soil sand content and increases with soil clay content. The graphic shows that the majority of the particles are scattered in the sandy zone with small particles are scattered elsewhere. As a result, we may conclude that there is no variance in the soil in the investigation because it is all sandy soil.

Experimental Determination of Natural Radioactivity in Soil and Measurement of Spot Background Gamma Radiation

The determination of natural radioactivity along with radium equivalent activity and the external and internal indices as well as measurement of spot background gamma radiation are presented in this paper. The results and discussion will be presented along with the details of findings from the selected areas of research.

The results obtained will be compared with worldwide averages whenever possible and whether certain readings reach critical values. For natural radioactivity measurement, soil samples are obtained from the Kurlok fault regions within regions of Kolasib District. The measurement for radium equivalent activity as well as external and internal hazard indices are measured from the natural radioactivity measurement. Lastly spot background gamma radiation is done on the fault area with gamma survey meter PM 1405.

The study area is located at north-east of India on Kolasib district in the state of Mizoram and extends from 23°53'29.57'' to 24°28'16.1'' latitude and 92°39'33.97'' to 92°48'40.71'' longitude as shown in figure 4.1.

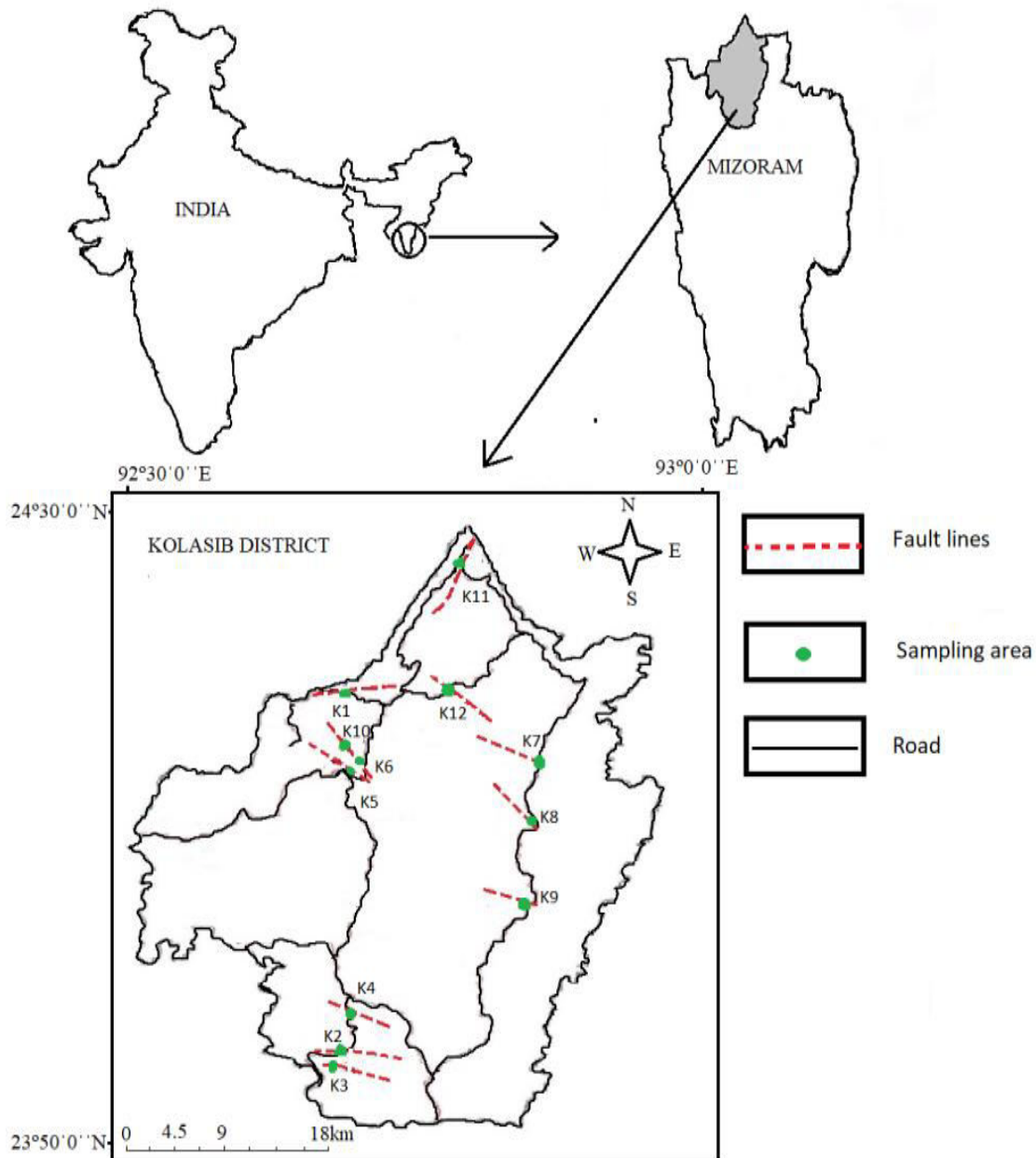


Figure 4.1: Geographical map for natural radioactivity measurement.

4.1 Determination of Natural Radioactivity in soil:

Measurement of natural radioactivity in soil is important as soil is the main contributor of natural radioactivity and radiation from the soil is considered to be the main source of irradiation on the human body (UNSCEAR 1993) (Chakiswa *et al.* 2001)

The current study estimates natural radioactivity using gamma spectrometry and a 5"x4" Sodium Iodide (NaI) detector doped with thallium (Tl). The radioactive concentrations of ^{238}U , ^{232}Th , and ^{40}K were assessed using this gamma spectrometer from soil samples taken

at the selected sampling locations within the study area of Mizoram's Kurlok fault regions of Kolasib districts. The spectrum obtained in this study is acquired and analysed using a personal computer-based 1K Multichannel analyzer GSPEC-SA linked with a detector.

4.1.1 Results and Discussion

Table 4.2: Activity Concentrations of ^{238}U , ^{232}Th and ^{40}K radionuclide in soil samples collected from fault regions of Kolasib District

SAMPLE CODE	ACTIVITY CONCENTRATION (Bq/kg)			Average
	^{238}U	^{232}Th	^{40}K	
K-1	12	34	615	220
K-2	32	89	774	298
K-3	36	101	858	331
K-4	51	141	1190	460
K-5	43	119	885	349
K-6	58	161	736	318
K-7	25	68	765	286
K-8	22	62	221	101
K-9	53	147	175	125
K-10	29	82	660	257
K-11	50	138	642	276
K-12	32	88	619	246



Figure: 4.2: Graph of Activity Concentrations of ^{238}U , ^{232}Th and ^{40}K radionuclide in soil samples collected from fault regions of Kolasib District

The measurement of Activity Concentrations of ^{238}U , ^{232}Th and ^{40}K radionuclide in soil samples collected from 12 different locations on fault regions of Kurlok fault areas of Kolasib District are given in table 1. These values show different variations when compared with each other as shown in figure 4.2. The activity concentrations collected from the soil samples were found to be in the range of 12 Bq/kg to 58 Bq/kg for ^{238}U , 34 Bq/kg to 161 Bq/kg for ^{232}Th and 175 Bq/kg to 1190 Bq/kg for ^{40}K . For ^{238}U , the average value is 37 Bq/kg with standard deviation of 14.1, for ^{232}Th the average value is 102 Bq/kg with standard deviation of 39 and for ^{40}K the average value is 678 Bq/kg with standard deviation of 274.4.

The average natural activity concentrations of ^{238}U , ^{232}Th and ^{40}K collected from the soil samples of 37 Bq/kg for ^{238}U , 102 Bq/kg for ^{232}Th and 678 Bq/kg for ^{40}K are compared with worldwide averages with values of 35 Bq/kg, 30 Bq/kg and 400 Bq/kg respectively (UNSCEAR 2000). It was seen that the values are higher than the worldwide averages when compared with each other. But on the other hand, these values are lower than IAEA critical values of 10,000 Bq/kg for ^{40}K and 1000 Bq/kg for all other radionuclides (IAEA,2004).

4.2: Estimation of Radium equivalent activity:

The values of radium equivalent activity for the soil samples were calculated using equation 2.7 and the values of external and internal hazard indices are calculated using equation 2.8 and equation 2.9. The calculated data for this is shown in table 4.3.

Table 4.3: Radium equivalent activity, External and internal hazard indices of ^{238}U , ^{232}Th and ^{40}K radionuclide in soil samples collected from fault regions of Kolasib District

SAMPLE CODE	Radium equivalent Activity (Bq/kg)	External Hazard Index (Hex)	Internal Hazard Index (Hin)
K-1	108	0.29	0.32
K-2	220	0.59	0.68
K-3	247	0.66	0.76
K-4	344	0.93	1.06
K-5	282	0.76	0.88
K-6	346	0.93	1.09
K-7	182	0.49	0.56
K-8	129	0.34	0.40
K-9	277	0.74	0.89
K-10	197	0.53	0.61
K-11	297	0.80	0.93
K-12	206	0.55	0.64

The measured values of Radium equivalent activity concentrations are within the range of 108 Bq/kg to 346 Bq/kg with an average value of 237 Bq/kg and standard deviation of 76.8. Radium equivalent activity concentration levels for the different regions have been found to be within the safe limit of 370 Bq/kg recommended by UNSCEAR (2000). Figure 4.3 shows the radium equivalent activity concentration in soil samples collected from fault regions of Kolasib District.

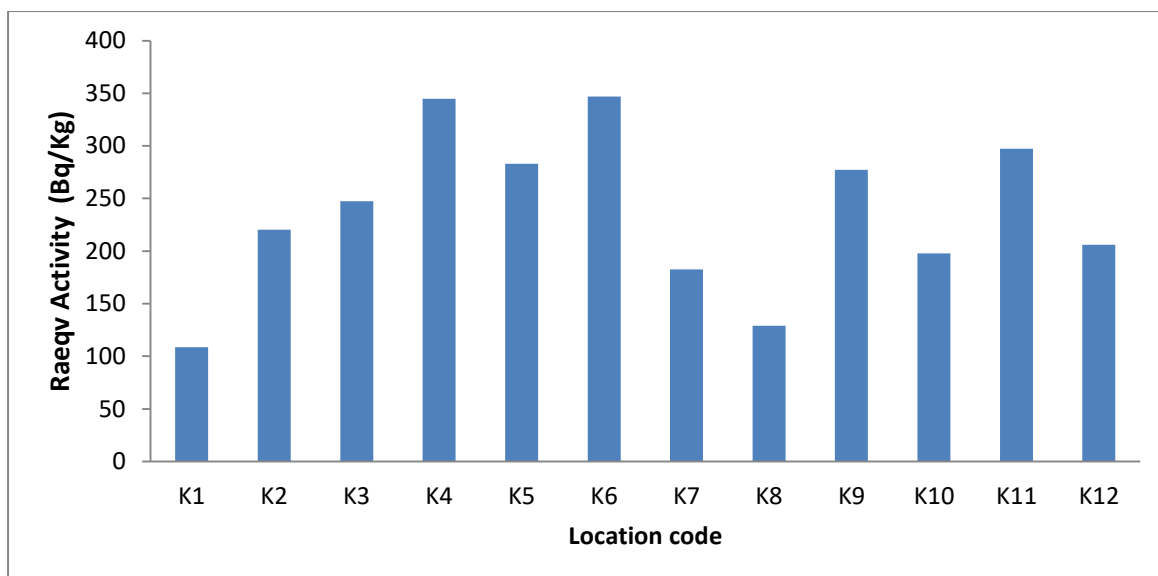


Figure 4.3: Radium equivalent activity concentration in soil samples collected from fault regions of Kolasib District.

4.3: Estimation of external and internal hazard indices

The values of external hazard index as well as internal hazard index are as shown in table 4.3. The values of the external hazard indices ranges from 0.29 to 0.93 with an average value of 0.63 and the values of internal hazard indices ranges from 0.32 to 1.09 with an average value of 0.74. Now soil from any region is considered safe and does not pose any radiological hazard if it does not exceed unity (Radiation Protection 112, 1999). The average values of both the external and internal hazard indices as seen from the results are less than unity and are considered safe. However only the values of internal hazard indices of K-4 and K-6 have values of 1.06 and 1.09 which are greater than 1. We can conclude that most of the soil from the regions are safe and can be used for construction materials. The distribution of external and internal hazard indices are as shown in figure 4.4.

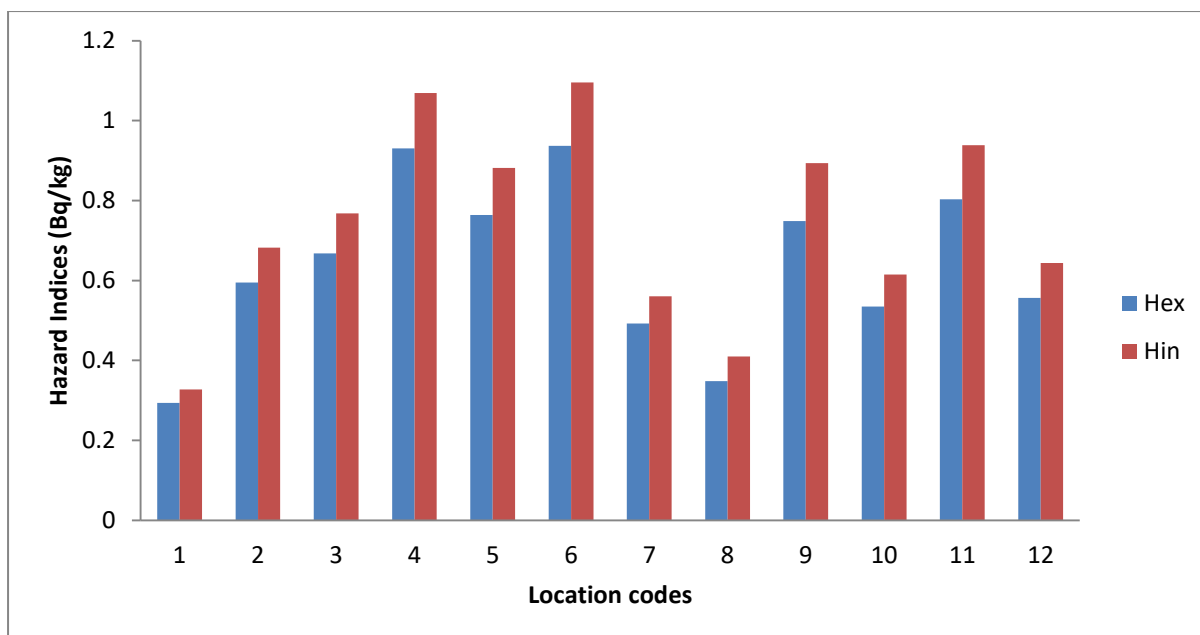


Figure 4.4: External and internal hazard indices of ^{238}U , ^{232}Th and ^{40}K radionuclide in soil samples collected from fault regions of Kolasib District.

4.4: Spot Background Gamma Radiation:

Background gamma radiation was taken at each spot of the fault regions where soil samples were collected. This was done with the help of gamma survey meter PM 1405 device. Measurement was taken in such a way that the survey meter was put 1 meter above the ground. This was done to assess the gamma radiation coming from terrestrial and cosmic origin. The latitudinal and longitudinal coordinates were measured at each sampling site with the help of a Global Positioning System (GPS) device. The results of values of background gamma radiation are as shown in table 4.4.

4.4.1 Results and Discussion:

Table 4.4: Background gamma radiation for fault regions of Kolasib district.

Location code	GPS Coordinate	Gamma Survey meter readings(nSv/hr)	Location code	GPS Coordinate	Gamma Survey meter readings(nSv/hr)
K1	Elevation 23 m N 24° 20' 45.23" E 092° 40'08.88"	106	K19	Elevation 48 m N 24° 20' 58.1" E 092° 45'32.0"	129
K2	Elevation 36 m N 24° 20' 51.39"	101	K20	Elevation 38 m N 24° 20' 57.5"	130

	E 092° 40'17.69"			E 092° 45'23.5"	
K3	Elevation 44 m N 24° 20' 58.15" E 092° 40'32.85"	107	K21	Elevation 37m N 24° 20' 59.0" E 092° 45'16.6"	105
K4	Elevation 260 m N 24° 15' 27.80" E 092° 40'36.50"	141	K22	Elevation 49 m N 24° 28' 11.5" E 092° 46'54.9"	120
K5	Elevation 351 m N 24° 15' 11.15" E 092° 40'37.48"	127	K23	Elevation 53 m N 24° 28' 16.1" E 092° 46'53.4"	127
K6	Elevation 431 m N 24° 14' 49.92" E 092° 40'56.08"	119	K24	Elevation 58 m N 24° 28' 15.7" E 092° 46'56.6"	145
K7	Elevation 385 m N 24° 14' 52.80" E 092° 41'36.26"	127	K25	Elevation 350m N 24° 14' 56.4" E 092° 41'12.3"	142
K8	Elevation 410 m N 24° 14' 59.27" E 092° 41'34.60"	89	K26	Elevation 360m N 24° 14' 55.2" E 092° 41'12.6"	130
K9	Elevation 403 m N 24° 14' 41.37" E 092° 41'24.56"	119	K27	Elevation 49 m N 24° 28' 11.5" E 092° 46'54.9"	157
K10	Elevation 474 m N 23° 53' 29.57" E 092° 40'23.97"	98	K28	Elevation 53 m N 24° 28' 16.1" E 092° 46'53.4"	127
K11	Elevation 468 m N 23° 53' 39.61" E 092° 40'25.25"	135	K29	Elevation 58 m N 24° 28' 15.7" E 092° 46'56.6"	92
K12	Elevation 447 m N 23° 54' 14.22" E 092° 40'26.09"	110	K30	Elevation 350m N 24° 14' 56.4" E 092° 41'12.3"	112
K13	Elevation 186 m N 23° 55' 59.81" E 092° 40'19.32"	132	K31	Elevation 360m N 24° 14' 55.2" E 092° 41'12.6"	106
K14	Elevation 138 m N 23° 56' 04.76" E 092° 39'46.88"	108	K32	Elevation 365m N 24° 14' 52.3" E 092° 41'11.8"	112
K15	Elevation 152 m N 23° 56' 00.50" E 092° 39'33.97"	102	K33	Elevation 679m N 24° 14'12.85" E092°48'26.37"	114

K16	Elevation 271 m N 23° 57' 59.14" E 092° 40'54.97"	89	K34	Elevation 695m N 24° 13'55.04" E092°48'24.42"	115
K17	Elevation 313 m N 23° 57' 19.59" E 092° 41'04.06"	109	K35	Elevation 683m N 24° 13'44.86" E092°48'17.95"	106
K18	Elevation 311 m N 23° 57' 11.55" E 092°41'06.12"	118	K36	Elevation 582m N 24° 12'06.28" E092°48'30.34"	111

As seen from the results, the values of spot background gamma radiation from fault regions of Kolasib district lines in the range of 89 nSv/hr to 157 nSv/hr. The minimum value 89 nSv/hr of background gamma radiation lies in the loactions K8 and K16 and maximum value of 157nSv/hr which lies in K27. The average value of the spot background gamma radiation from all the regions is 117 nSv/hr with standard deviation of 16. In comparison to the values provided by UNSCEAR (2000) for different nations (mean of 59 nGy/h in the range of 18- 93 nGy/h), the background gamma radiation levels obtained were all found to be higher. But these values were within the given range of background gamma levels for India (89 nGy/h in the range of 27–3051 nGy/h) as reported by Nambi *et al.* (1986).

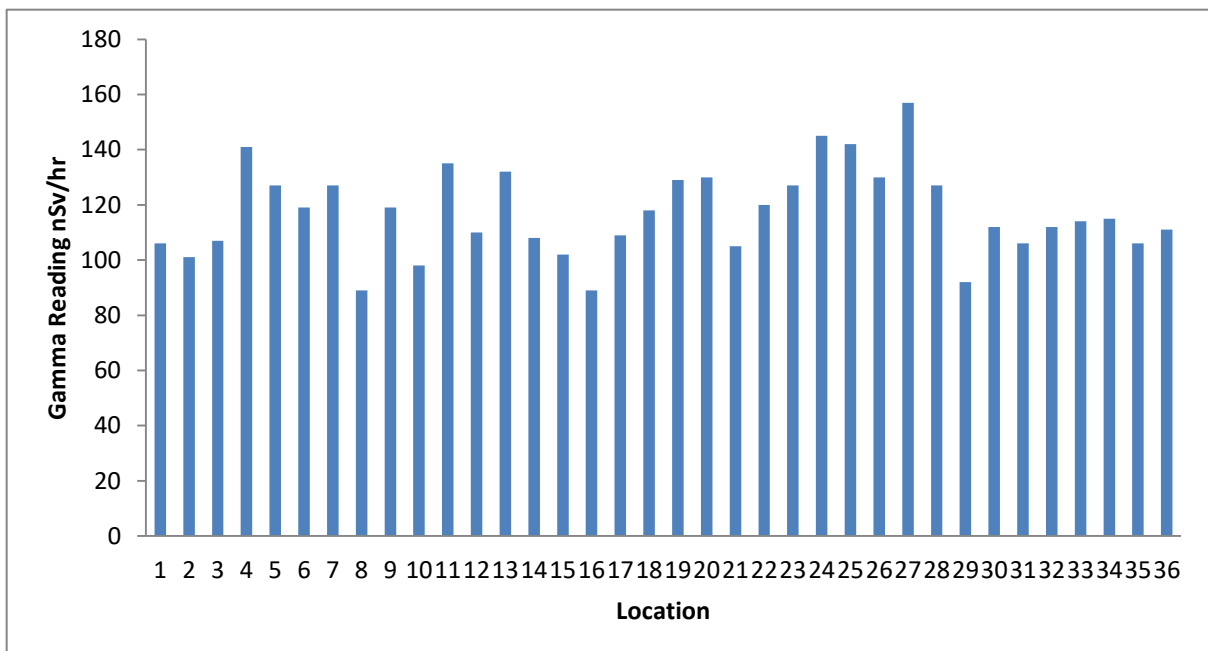


Figure 4.5: Background gamma radiation for fault regions of Kolasib district.

Table 4.5 shows the background gamma radiation from only Kurlok fault regions. It was seen that the values of background gamma radiation values ranges from 89nSv/hr to 145nSv/hr with an average value of 120 nSv/hr. The average values of Kurlok when compared with the values from all the fault regions of the district shows that the values lie in the same ranges and no significant variation is seen as the faults are all located within the district. Figure 4.6 shows the distribution of background gamma radiation of Kurlok faults.

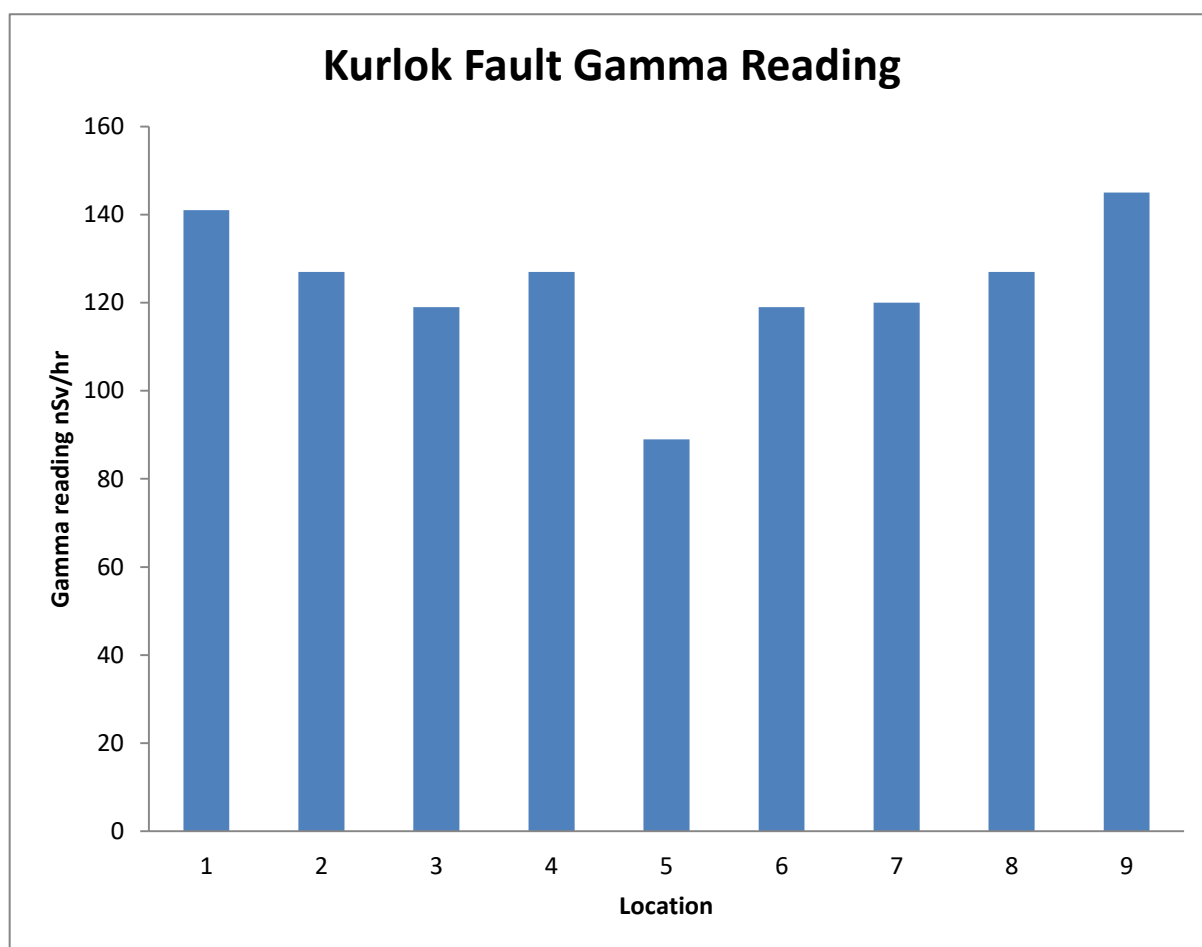


Figure 4.6:Background gamma radiation for only Kurlok fault regions

4.5: Correlation between Gamma and radium equivalent activity:

Figure 4.7 shows the correlation between radium equivalent activity and background gamma radiation from fault regions of Kolasib district. A very poor correlation was between the two measured parameters was obtained. The lack of correlation could be attributed to the fact that cosmic radiations contribute to the background gamma level recorded at each sample

site. The background gamma radiation measured using the gamma survey meter measures the gamma radiations coming from both terrestrial and cosmic sources. Furthermore, only the activity concentration measured from three terrestrial radionuclides, namely ^{238}U , ^{232}Th , and ^{40}K , is accounted for by the radium equivalent activity. There may also be other gamma-emitting terrestrial radionuclides that contribute to the background gamma level but were not considered when calculating the radium equivalent activity.

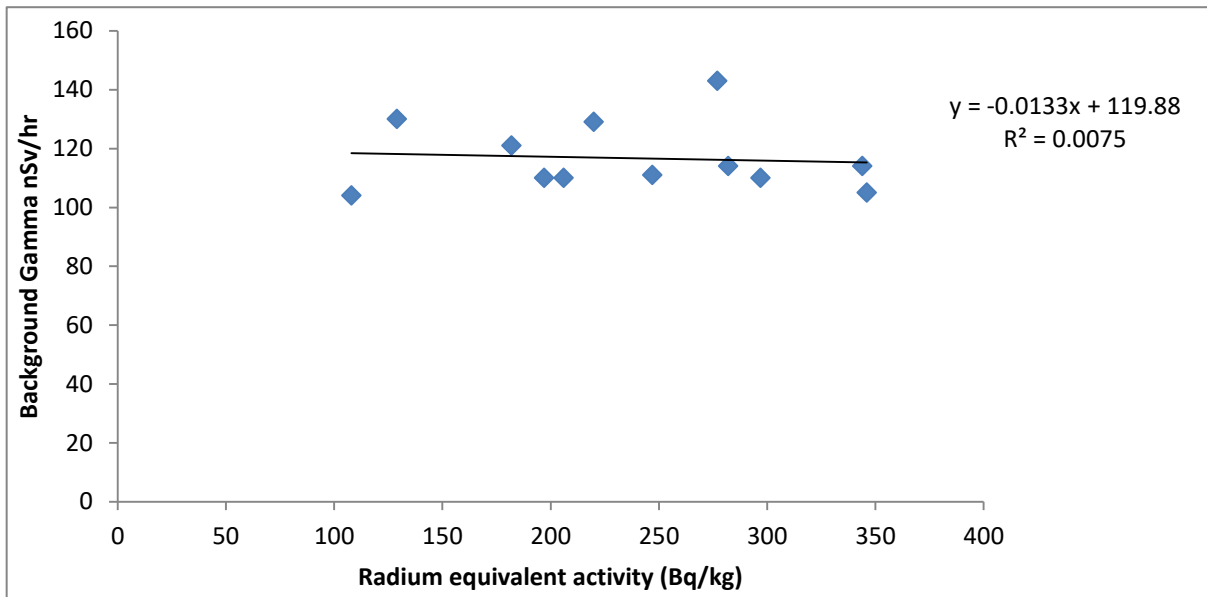


Figure 4.7:Correlation between background gamma level and radium equivalent activity
In fault regions of Kolasib District.

CONCLUSIONS

This chapter will give details on the conclusions drawn out from the thesis titled, “Measurement of radon exhalation and its modelling along Kurlok fault regions of Kolasib district, Mizoram”. This study was carried out to get a baseline data for future studies and to get a better understanding of the different properties of radionuclides in the soil especially in fault regions. The study of radon and its exhalation would provide data for the properties and activity within the soil and in faults. Along with this the activity concentration studies is significant in providing the impact of natural radionuclides towards human health.

- The study areas lie in Kolasib district of Mizoram which is situated north of the capital Aizawl. The areas extend from 92° 30' 0'' E to 93° 0' 0'' E longitude and 24° 30' 0'' N to 23° 50' 0'' N latitude. Three locations for each fault is selected in which soil samples are collected. The collected soil samples are then measured using scintillation based Smart RnDuo device. The measurement of mass exhalation was carried out in 36 different locations of Kolasib district in which the values ranges from 2.3 mBqkg⁻¹hr⁻¹ – 45.7 mBqkg⁻¹hr⁻¹ with an average of 20.42 mBqkg⁻¹hr⁻¹. The results obtained from this are comparable to work done in Northern Rajasthan with an average value of 14.96 mBq/kg/hr (V. Duggal *et al.* 2015), Kangra District, Himachal Pradesh with an average value of 19.91 mBq/kg/hr (D.K. Sharma *et al.* 2003) and Kathmandu Valley, Nepal with an average value of 6.4 mBq/kg/hr (P. Parajuli *et al.* 2015). For comparison, measurements were also taken from some selected fault regions of Aizawl district which ranges between 11.2 mBq/kg/hr - 72.2 mBq/kg/hr with an average of 39.92 mBq/kg/hr and standard deviation of 13.5 mBq/kg/hr. The results in different regions may vary because rainfall, snowfall, freezing and increase in atmospheric pressure results in decrease of exhalation rate, whereas increase in wind speed and temperature can increase it. Also radon exhalation increases with moisture

content upto 8% and starts decreasing if water content is increased further (Faheem M, 2008) (Hosada *et al* 2007).

- The measured and calculated values have been compared for modeling purpose with the help of UNSCEAR equation. The calculated values lies within the range of 4.21 mBq/kg/hr to 31 mBq/kg/hr with an average value of 18.7 mBq/kg/hr and standard deviation of 9.44 mBq/kg/hr. With an average of 1.07, the ratio between estimated and measured values ranges from 0.39 to 3.86. We can observe from the findings that the measured values are greater in some places and the estimated values are higher in others. As previously stated, soil moisture content, as well as the geology of the area, play a crucial part in exhalation. Exhalation rates are influenced by a variety of factors, including porosity, temperature, and humidity. Artificial structures inside the soil, such as pipes, can sometimes impact the flow of radon within the soil (Hosoda *et al.* 2009). If the measurements were collected in a more controlled environment, the comparison approach would be more appropriate.
- Radon concentration in soil gas is carried out on the spot of the study areas with Smart RnDuo connected to a soil probe. Radon gas concentrations are monitored on the ground at depths of 60 cm, 90 cm, and 120 cm along the Kurlok fault regions, and the other faults within Kolasib district for comparison purposes. The study region is located between 24° 11' 08.93" and 24° 20' 58.15" latitude and 92° 40' 32.85" to 92° 48' 34.25" longitude, with elevations ranging from 36 m to 568 m above sea level. The average values of radon concentration in soil gas at the Kurlok Fault zones were 5.93 kBq/m³ at 120 cm depth, 2.93 kBq/m³ at 90 cm depth, and 0.13 kBq/m³ at 60 cm depth represented by K1, K2, and K3. In the remaining sections (K4-K7), the average radon concentration in soil gas was 3.77 kBq/m³ at 120 cm depth, 1.9 kBq/m³ at 90 cm depth, and 0.12 kBq/m³ at 60 cm level. The average concentration of soil gas in the Kurlok fault zones is higher than in the other districts. This may be due to the Kurlok fault having a larger or longer fault line that runs through the intersections. Because radon is

dependent on faults for transit through rocks beneath the earth, it is expected to be more concentrated in areas with more faults. The results from this present investigation is compared with results from recent work done by other investigators and was found to be well within the ranges of results from South Kumaun Lesser Himalayas with concentration values of 1.10–31.80 kBq/m³(Prasad *et al.*2008), Garhwal Himalaya with concentration values of 0.01–2.33kBq/m³ (Bourai *et al.*2013) and northern Rajasthan with concentration values of 0.09-10.40 kBq/m³(Vikas Duggal *et al.*2014).

- The radon concentration in soil gas measured was found to be maximum at depths of 120cm when compared with depths of 90cm and 60cm. Thus we can conclude that radon concentration in soil gas increases as we go further towards the depth of the soil and hence the concentration increases with increase in the depth. This trend follows the same trend as measurements done by Duggalet *al.* (2014), Hasan *et al.* (2001) and Kaur *et al.*(2015).
- Soil grain size determination is important in assessing the type of soil present in the areas of study. This was carried out with a mechanical sieve shaker with different mesh sizes. It was observed that the more than 90% of the grain size distribution falls under ‘Sand’ category while the rest are distributed in ‘Silt’ and ‘Clay’. This was again plotted using USDA triangular plotting with the help of ‘Origin’ software. It was concluded that all the soil from the study areas are of sandy type of soil.
- The measurement of natural radioactivity in soil is important since soil is the primary source of natural radioactivity. This is done with the help of a 5"x4" Sodium Iodide (NaI) detector doped with thallium (Tl). The radioactive concentrations of ²³⁸U, ²³²Th, and ⁴⁰K were assessed from soil samples collected from the study areas. The spectrum is analysed using a personal computer-based 1K Multichannel analyzer GSPEC-SA linked with the detector. The values of activity concentrations of ²³⁸U, ²³²Th and ⁴⁰K radionuclide in soil samples collected from 12 different loactions on fault regions of Kurlok fault areas of Kolasib District were found to be in the range of 12 Bq/kg to 58 Bq/kg for ²³⁸U, 34 Bq/kg to 161 Bq/kg for ²³²Th and 175

Bq/kg to 1190 Bq/kg for ^{40}K with an average of 37 Bq/kg, 102 Bq/kg and 678 Bq/kg for ^{238}U , ^{232}Th and ^{40}K respectively. These values when compared with the worldwide values seems to be slightly higher but are lower than the IAEA (2004) critical values.

- The values of Radium equivalent activity were obtained from values of the activity concentrations and lies within the range of 108 Bq/kg to 346 Bq/kg with an average value of 237 Bq/kg. This value does not exceed the safe limit of 370 Bq/kg recommended by UNSCEAR (2000). The values of hazard indices are calculated from the activity concentration values. The values of the external hazard indices ranges from 0.29 to 0.93 with an average value of 0.63 and the values of internal hazard indices ranges from 0.32 to 1.09 with an average value of 0.74. Two locations have values exceeding 1, but the rest are within the safe limit according to Radiation Protection 112(1999). But the overall averages are all below unity and hence can be considered to be safe and not pose any radiological hazard. The soil from this region can be considered to be safe and can be used for construction materials.
- Spot background gamma radiation measurement was carried out on the fault areas in which soil samples were collected. This was done with the help of gamma survey meter PM 1405 device. The radiation values lies in the range of 89 nSv/hr to 157 nSv/hr with an average of 117 nSv/hr. These values were a bit higher than values provided by UNSCEAR (2000) but were well within the ranges for India. Correlation between background gamma level and radium equivalent activity in fault regions of Kolasib District was plotted. A very poor correlation was observed which could be attributed to the fact that cosmic radiations contribute to the background gamma and only the activity concentration measured from three terrestrial radionuclides, namely ^{238}U , ^{232}Th , and ^{40}K , is accounted for by the radium equivalent activity. There may also be other gamma-emitting terrestrial radionuclides that contribute to the background gamma level but were not considered when calculating the radium equivalent activity.

- The results obtained from this study were all from fault regions of Kurlok and other fault regions of Kolasib district. Data obtained from this study would be helpful in providing baseline data for future studies. For each of the different methods mentioned in this thesis, comparison analysis could be further implemented if non fault areas of the district were covered. This would help in assessing information regarding differences between faults and non fault regions of the areas.

APPENDICES

APPENDIX – I

Protocol for measurement of Radon mass exhalation

The radon mass exhalation rate controls the radon emission potential of a sample (Jm). The Can technique, Lucas cell coupled chamber method, online monitor coupled chamber method, and other technologies are available for measuring radon emission from building materials. Because of concerns with leakage and thoron interference in radon measurement, the can technique has limitations in terms of accuracy of estimated radon exhalation rate. As a result, it is advised that this procedure not be used indefinitely. Because just one measurement value is used for calculation, the Lucas cell connected chamber approach has limitations in terms of determined radon exhalation accuracy. As a result, the online monitor coupled chamber method is the optimum method for determining radon exhalation from building materials and NORM samples.

The Protocol for measurement of Radon Mass exhalation is given as:

- The Smart RnDuo measurement instrument includes a 'Mass Exhalation Chamber' for measuring mass exhalation volume.
- The spent scintillation cell is replaced with one that is maintained for at least 3 hours following radon flushing to ensure that it is clear of background.
- The Smart RnDuo is turned on, the cycle is set to 1 hour, and the Pump is turned off for Diffusion Mode.
- For diffusion mode, connect and link the Smart RnDuo and the mass exhalation chamber using the signal connection shown in Figure 2.4.
- The amount of soil in the accumulation chamber should be at its maximum.
- After encapsulating the soil, the radon concentrations are tested for 1 hour cycles throughout a 24-hour period.

APPENDIX-II

Protocol for measurement of radon concentration in soil gas

A soil probe and an online radon monitor can be used to measure radon concentration in soil gas. Humidity should cause the least amount of disturbance in the online monitor. In this case, soil gas measurement with RnDuo is a viable alternative. The methodology for measuring soil gas radon using RnDuo at various depths from the soil surface is explained below.

Deployment Protocol

- To test the radon gas concentration in soil pore space, use the 'soil probe' that comes with the RnDuo system. Before utilising the probe, make sure the inner pipe is inserted and the probe head is attached to it.
- By hammering on the probe head, you may get the probe to the appropriate depth. If the probe encounters further resistance, a rock may be encountered; in this case, modify the insertion site since the probe tip may be damaged.
- Remove the probe head and inner pipe once the probe has been placed to the desired depth. Replacing the probe head with a sample head connected to the inner sampling pipe is a good idea. Ascertain that the connection between the sample head and the probe is leak-proof.
- Connect RnDuo monitor to the inlet port of the soil probe using flexible tubing. Close the outlet port of the probe with rubber cap to seal it.

Measurement Protocol

- Turn the pump on manually for 2-3 minutes by putting Pump setting = On in Rn222 mode
- For measurement of radon set up the parameters as below and start the measurement. Mode = Rn222 Modify cycle = 15 minutes Pump Settings = Off
- Continue the measurement upto 1 hour for each depth. Ignore the first reading in each case while taking average

- For measurements at subsequent depths the RnDuo monitor should not be turned Off. Instead the probe should be hammered to the next depth level and the measurement procedure given above be repeated
- The sequence of measurement should be in an increasing order of depth.
- Measurement of radon concentration in soil gas should be performed such that, the difference in two depth levels is at least 15 cm to avoid dilution.
- Ideally, soil gas measurements should be carried out up to a depth of 120 cm.

APPENDIX-III

Energy Calibration of NaI (TI) Spectrometer using ¹³⁷Cs and ⁶⁰Co sources

Procedure:

- Connect the NaI(Tl) detector to GSPEC-SA which is connected to Desktop computer through a USB port
- After turning on the system, open the Spectrum Acquisition & Analysis software in the computer. Open the 'Set Parameter' from the drop-down 'Acquisition' and set the parameter as follow:
Set HV – 650 V, Gain -6, LLD-1
- We receive a ¹³⁷Cs peak of energy 661.99 keV at Channel number 231, a ⁶⁰Co peak of energy 1173 keV at Channel number 403, and a ⁶⁰Co peak of energy 1332.01 keV at Channel number 455, thanks to this parameter value from the GSPEC-SA specification.
- In the 'Acquisition' drop down within the 'Control,' change the Preset Time to your desired value (500 s in our example). To begin acquiring the spectrum, click the 'Start Acquisition' button.
- After the acquisition period has passed, go to the 'ROI' drop-down menu and choose the region of interest (ROI) for each peak in the spectrum. Then, from the 'ROI' drop down, select 'ROI Analysis' and 'SAVE/PRINT' the analysis report.
- To calibrate the system, select 'Math Functions' from the drop-down menu and select 'Calibration.' Choose '3 Point Calibration' from the 'Type' drop-

down menu. Enter the values for 'Centroid 1' and 'Energy' from the ROI analysis report in the 'Data' box, then click 'Accept' from the 'Valid Peaks' box. Carry on with Centroid 2 and Centroid 3 in the same way. 'Calibrate Spectrum' and 'Close' are the two options. At this moment, the calibration is complete.

- After the calibration operation is completed, go to the 'Math Functions' drop down and select 'Calibration.' The calibration result will be displayed at the bottom of the screen, $m_1 = 3.4608$, $m_2 = 0$, and $c = -20.644$.

APPENDIX – IV

Efficiency Calibration using 40K (RGK-1), 238U (RGU-1) & 232Th (RGTh-1)IAEA Standard Sources

Procedure:

- Connect the NaI (TI) detector to GSPEC-SA which is connected to Desktop computer through a USB port.
- After turning on the system, open the Spectrum Acquisition & Analysis software in the computer. Open the 'Set Parameter' from the drop-down 'Acquisition' and set the parameter as follow: SET HV – 650V; GAIN6; LLD – 1

This parameter value came with the GSPEC-SA specification so that we get ¹³⁷Cs peak of energy 661.99 keV at Channel number 231, ⁶⁰Co peak of energy 1173 keV at Channel number 403 and ⁶⁰Co peak of energy 1332.01 keV at Channel number 455.

- Set the Preset time so that photo peaks have sufficient counts for analysis by going to 'Acquisition' of the 'Control' drop down. (10800 s in our case).
- You can start acquiring the spectrum either by going to 'Acquisition' drop-down and press 'Start' or by going to 'Control' and press 'Start Acquisition'.

- After acquisition time is over, go to the drop-down 'ROI' where the region of interest (ROI) of each peak of the spectrum can be select. After this, click the 'ROI Analysis' from the 'ROI' drop down and 'SAVE/PRINT'the analysis report.
- Taking 238U source as an example, let us choose 214Pb (which is one nuclide in 238U decay series) as a nuclide for efficiency calibration. Here we can choose any nuclide of the 238U decay series, but it should be noted that it is also present in the Possible Isotopes in ROI of the soil sample analyzed.
- Note down the 'Centroid (keV)' and 'Area' from the ROI analysis report.
- Go to 'Utilities' drop down and click 'Gamma Library' and search for 214Pb. Of all the isotope of 214Pb, choose the one with energy closest to 'Centroid (keV)' and note down the branching intensity.
- Calculte the efficiency of each source using equation 2.5

APPENDIX – V

Operation of Survey Meter PM 1405

- The operation is carried out by four buttons: left, right, upper and lower. The detector window could be opened by shifting the screen-filter Operating mode, current state of the instrument, as well as the key functions for changing the instrument state are indicated on the LCD. For example, on LCD near to the title designating forthcoming action, such as "BACK", "SELECT", "MEMORY" etc., is displayed the image of arrows.
- The arrow points to the key, which is to be pressed to enter chosen operating mode. For example, if the arrow points to the left it is necessary to press the left button, if upwards – it is necessary to press the upper button.
- The instrument enters DER measurement mode automatically just after switching on or purposely from "MENU". For that it is necessary to choose the "MEASUREMENT γ " line and press the "SELECT" button.
- Being in the DER mode the instrument displays on LCD continuously

measured values the photon radiation DER in " $\mu\text{Sv/h}$ ", " mSv/h " and the statistical error of the measured DER in percentage.

- On reaching 15 % and less of statistical error DER could be readout. And the longer is the measurement time the smaller will be the statistical error. Measured DER value could be stored in the non-volatile mamory after pressing the "MEMORY" button.
- If the statistical error is more than 10 % on the LCD is indicated the information, if the statistical error is less than 10 % on the LCD are indicated the measurement results. To store the measurement results it is necessary to press the "YES" button

References

- Agarwal, Chhavi (2011). Nondestructive assay of nuclear materials by gamma ray spectrometry. (Doctoral dissertation, Homi Bhabha National Institute).
- Amit Kumar, Chauhan, R.P., Manish Joshi, Sahoo, B.K., (2014). Modelling of indoor radon concentration from radon exhalation rates of building materials and validation through measurements. *J. Environ. Radiact.*, **27**, 50-55.
- Beretka J, Mathew PJ (1985). *Health Phys* **48(1)**, 87-95, DOI: 10.1097/00004032-198501000-00007.
- Bourai AA, Aswal S, Dangwal A, Rawat M, Prasad M, Naithani Prasad N, Joshi V and Ramola RC. 2013 Measurement of radon flux and soil-gas radon concentration along the main central thrust, Garhwal Himalaya, using SRM and RAD7 detectors. *Acta Geophys*; **61(4)** 950–957.
- Bureau International des Poids et Mesures Table of Radionuclides (2004). Monographie BIPM-5.
- Chikasawa K, Ishii T, Ugiyama H (2001). Terrestrial gamma radiation in Kochi Prefecture, Japan. *J Health Sci*, **47**, 361-372.
- Choubey VM, Sharma KK, Ramola RC. Geology of radon occurrence around Jari in Parvati valley, Himachal Pradesh, India. *J. Environ. Radioact.* 1997; **34(2)**:139-147.
- D.K. Sharma, A.Kumar, M. Kumar and S. Singh. Study of uranium, radium and radon exhalation rate in soil samples from some areas of Kangra district, Himachal Pradesh, India using solid-state nuclear track detectors. *Radiation Measurements*. (2003); **36(1-6)**, 363-366
- Darby S, et al. (2005). Radon in homes and risk of lung cancer: collaborative analysis of individual data from 13 European case-control studies. *BMJ*, **330(7485)**, 223-227.

- Duenas, C., Fernández, M. C., Carretero, J., Liger, E., and Pérez, M. (1997, February). Release of ^{222}Rn from some soils. *Annals of Geophysics*, **15(1)**, 124-133. Springer Berlin/Heidelberg.
- Duggal V, Rani A and Mehra R. 2014 Measurement of soil-gas radon in some areas of northern Rajasthan, India. *J. Earth Syst. Sci.*; **123(6)**:1241-1247
- Duggal, V., Mehra, R., and Rani, A. (2015). Study of radium and radon exhalation rate in soil samples from areas of northern Rajasthan. *J. Geol. Soc. Of India*, **86(3)**, 331-336.
- EC-European Commission. Radiological protection principles concerning the natural radioactivity of building materials. Radiat. Prot. 112.(1999)
- Faheem, M. (2008). Radon exhalation and its dependence on moisture content from samples of soil and building materials. *Radiation Measurements*, **43(8)**, 1458-1462.
- Frank, A. L., and Benton, E. V. (1977). Radon dosimetry using plastic nuclear track detectors. *Nucl. Track Det.*, **1(3-4)**, 149-179.
- García-Gaines, Rubén A., Frankenstein, Susan, (2015). USCS and the USDA Soil Classification System: Development of a Mapping Scheme. ERDC/CRREL TR-15-4. 5-7.
- Hafez, A. F., El-Khatib, A. M., Moharram, B. M., Kotb, M. A., and Abdel-Naby, A. (1991). Field Measurements of Radon Exhalation and Ra-226 Content in Soil using the Can-Technique. *Isotopenpraxis Isot. Env. and Health Studies*, **27(4)**, 188-190
- Hasan AK, Subber ARH, Shaltakh AR. Measurement of radon concentration in soil gas using RAD7 in the environs of Al-Najaf Al-Ashraf City-Iraq. *Adv. Appl. Sci. Res.* 2001; **2(5)**:273-278.

- Hassan Nabil M, Tokonami Shinji, Fukushi Masahiro (2011). A simple technique for studying the dependence of radon and thoron exhalation rate from building materials on absolute humidity. *J Radioanal Nucl Chem*, **287**, 185-191, DOI 10.1007/s10967-010-0665-7.
- Hosoda, M., Shimo, M., Sugino, M., Furukawa, M., & Fukushi, M. (2007). Effect of soil moisture content on radon and thoron exhalation. *Journal of nuclear science and technology*, **44(4)**, 664-672.
- Hosoda, M., Sorimachi, A., Yasuoka, Y., Ishikawa, T., Sahoo, S. K., Furukawa, M., ... & Uchida, S. (2009). Simultaneous measurements of radon and thoron exhalation rates and comparison with values calculated by UNSCEAR equation. *Journal of radiation research*, **50(4)**, 333-343.
- Hussain H. H., Hussain, R. O. , Yousef, R. M. , Shamkhi Q. (2009): Natural radioactivity of some local building materials in the middle Euphrates of Iraq 2009, DOI 10.1007/s10967-010-0464-1
- IAEA, I. Safety Standards Series: Application of the Concepts of Exclusion, Exemption and Clearance: Safety Guide No. RS-G 1,7.(2004)
- IARC (1988). Man-made mineral fibres and radon. Lyon: International Agency for Research on Cancer. IARC Monographs on the Evaluation of Carcinogenic Risks to Humans, **43**
- Ibrahim SA, Wrenn ME, Singh NP, Cohen N, Saccomano G (1983). Thorium concentrations in human tissues from two U.S. populations. *Health Physics*, **44(1)**, 213-220.
- International Standard, ISO 18589-3:2007(E), 7.3.1. Energy calibration.
- Jacobi W (1993) The History of the Radon Problems in Mines and Homes, *Ann. ICRP*, **23**, 39-45.

- Jaishi, H. P., Singh, S., Tiwari, R. P., and Tiwari, R. C. (2014). Analysis of soil radon data in earthquake precursory studies. *Annals of Geophysics*, **57(5)**, S0544.
- Jaishi, H. P., Singh, S., Tiwari, R. P., and Tiwari, R. C. (2015). Soil-gas Thoron Concentration Associated with Seismic Activity. *Chiang Mai J. Sci.*, **42(4)**, 972-979.
- Kalyani, V.D.M.L., Chandrashekar Rao, M.U.S., Sree Krishnamurthy, G., Satyanarayana G. Sastry, D.L., Sahasrabhude, S.G., Bagu, D.A.R., and Iyer, M. R., (1990). Analysis of Th-232 and U-238 in the beach sands and the ocean
- Kannan, V., Rajan, M.P., Iyengar, M.A.R., Ramesh, R., (2002). Distribution of natural and anthropogenic radionuclides in soil and beach sand samples of Kalpakkam (India) using HPGe gamma ray spectrometry. *Appl. Radiat. Isot.*, **57**, 109-119.
- Kaur N, Singh A, Kaur M, Dhaliwal AS. Measurements of Radon gas Concentration in Soil. *Int.J. Comput.Appl.*2015;975:8887
- Kerur, B.R., Rajeshwari, T., Nagabhushana, N.M., Anil Kumar, S., Narayani, K., Rekha, A.K., Hanumaiah, B., (2011). Natural radioactivity levels in some environmental samples of Shapur region of north Karnataka, India. *Radiat. Prot. Environ.*, **34(1)**, 55-59.
- Kumar Rajesh, Senagupta, D., Rajendra Prasad, (2003). Natural radioactivity and radon exhalation studies of rock samples from Surda Copper deposits in Singhbhum shear zone. *Radiat. Meas.*, **36**, 551-553.
- Lekshmi R, Arunima S, Jojo PJ (2018). Determination of Radon Exhalation Rates and Emanation Factor of Some Soil Samples Collected From Southern Seashore of Kerala, India. *JUSPS-A*, **30 (1)**, 80-85.
- M. Faheema and Matiullah. Radon exhalation and its dependence on moisture content from samples of soil and building materials. *Radiation Measurements*(2008);**43(8)**,1458-1462

- Mahur, A.K., Rajesh Kumar, Sonkawade, R.G., Senagupta, D., Rajendraprasad, (2008). Measurement of natural radioactivity and radon exhalation rate from rock samples of Jaduguda uranium mines and its radiological implications. *Nucl. Instru. & Meth. Phys. Res., B* **266**, 1591-1597.
- Majumdar, D.(2000) Radon: Not so Noble, *Resonance*,**5(7)**,44-55
- Manjunatha, S., Jayasheelan, A., Venkataramaiah, P., (2013). Study of distribution of ²²⁶Ra, ²³²Th and ⁴⁰K in different rock formations and their dose estimation in and around chickmagalur, India. *Int. J. Radiat. Res.*, **11(3)**, 183-187.
- Mujahid SA, Hussain S, Ramzan M (2010). Measurement of radon exhalation rate and soil gas radon concentration in areas of southern Punjab, Pakistan. *Radiation Protection Dosimetry*, 1-4. doi:10.1093/rpd/ncq119.
- Nagaratnam A (1994), Radon: A Historical Overview, *Bull. of. Rad. Prot.*, **17**, 1-10.
- Nambi KS, Bapat VN, David M, Sundaram VK, Santa CM, Soman SD, (1986).Natural Background Radiation and Population Dose Distribution in India. India:HPD, BARC.
- Nezmal, M., Matolín, M., Just, G., and Turek, K. (2004). Short-term temporal variations of soil gas radon concentration and comparison of measurement techniques. *Radiat. Prot. Dosim.*, **108(1)**, 55-63.
- NRC (National Research Council) (1988), Health risks of radon and other internally deposited alpha-emitters. National Research Council, Washington, DC, National Academy Press.
- Parajuli, P., Thapa, D., and Shah, B. R. (2015). Study of radon exhalation rate in soil samples of Kathmandu valley using passive detector LR115. *Intl. J. Chem. Phys. Sci.*, **4(4)**, 30-9.
- Peterson John, MacDonell Margaret, Haroun Lynne, Monette Fred (2001). Radiological and Chemical Fact Sheets to Support Health Risk Analyses for

Contaminated Areas, Argonne National Laboratory Environmental Science Division. 2007 Mar, 133.

Prasad, Y., Prasad, G., Gusain, G. S., Choubey, V. M., and Ramola, R. C. (2008). Radon exhalation rate from soil samples of South Kumaun Lesser Himalayas, India. *Radiat. Meas.*, **43**, S369-S374.

Quindos, L. S., Fernandez, P. L. and Soto, J. Building materials as source of exposure in houses. In: Indoor Air 87, Vol. 2. Seifert, B. and Esdorn, H., Eds. Institute of Water, Soil and Hygiene, p. 365 (1987).

Ramachandran TV, Mayya YS, Sadashivan S, Nair RN, Eappen KP (2003). Radon-Thoron Levels and Inhalation Dose Distribution Patterns in Indian Dwellings. BARC Report, BARC/2003/E/026. Bhabha Atomic Research Centre, Mumbai, Government of India, 1-43.

Ramola, R., and Choubey, V. (2003). Measurement of radon exhalation rate from soil samples of Garhwal Himalaya, India. *J. of Radio. and Nucl. Chem.*, **256(2)**, 219-223.

Rekhakutty, R., Sahasrabudhe, S.G., Chakraborty, P.P., Iyengar, T.S., Iyer, M.R., Narayana, Y., Siddappa, K., (1993). A relative comparison of activities due to U and Th daughters products and its concentration in soils from different regions. *Bulletin of Radiat. Prot.*, **16**, 144-150

Rohmingliana P.C., Vanchhawng Lalmuanpuia. Measurement of indoor concentrations of radon and thoron in Mizoram, India (2010). *Sci Vis* **10 (4)**, 148-152

Rohmingliana PC, Vanchhawng Lalmuanpuia, Thapa RK, Sahoo BK, Singh OP, Zoliana B, Mayya YS (2009). Measurement of Indoor Radon and Thoron Concentrations in Correlation to Geographical Location and Construction types of Buildings in Mizoram.(with special reference to Aizawl, Champhai and Kolasib districts). Proc. VIth Conference of Physics Academy of North East, Tripura University, April 3-4.

- Sahoo BK, Nathwani Dipen, Eappen KP, Ramachandran TV, Gaware JJ, Mayya YS (2007). Estimation of radon emanation factor in Indian building materials. *Radiation Measurements*, **42**, 1422-1425.
- Sarma, H. K., Deka, P. C., Sarkar, S., Goswami, T. D., and Sarma, B. K. (2011). Radon activity and radon exhalation rates from some soil samples by using SSNTD. In *Proc. Of The Sevnt. Ntnl. Symp. On Sol. Stat. Nucl. Track Det. And Their Appl.: Abst. and Souv.*, **2(10)**, 5024-5029
- Shashikumar, T. S., (2010). Studies on radon in soil gas and its concentration in the atmosphere. A thesis submitted to University of Mysore, Mysuru.
- Singh, S., Jaishi, H. P., Tiwari, R. P., and Tiwari, R. C. (2016). A study of variation in soil gas concentration associated with earthquakes near Indo-Burma Subduction zone. *Geoenviron. Disast.*, **3(1)**, 22.
- Srivastava Alok, Lalramengzami R, Laldawngliana C, Sinha C, Ghosh S, Dwivedi KK, Saxena A, Ramachandran TV (1996). Measurement of Potential Alpha Energy Exposure (PAEE) of Radon and its Progenies in Dwellings in the North-Eastern Region of India. *Radiat. Meas.*, **26**, 291-295.
- Stranden E, Kolstad A, Lind B (1984). Radon exhalation: Moisture and temperature dependence. *Health Physics*, **47(3)**, 480-484.
- Sun, K., Guo, Q., and Cheng, J. (2004). The effect of some soil characteristics on soil radon concentration and radon exhalation from soil surface. *J. of Nucl. Sci. and Tech.*, **41(11)**, 1113-1117.
- Thuamthansanga, T., Sahoo, B. K., Tiwari, R. C., & Tiwari, R. P. (2021). Study of meteorological influence on the count of ^{222}Rn and ^{220}Rn gases and its possibility for a forecasting gas. *Radiat Environ Med*, **10(1)**, 37-47.
- UNSCEAR (1993) United Nations Scientific Committee on the Effects of Atomic Radiation., Sources, Effects and Risks of Ionizing Radiation., Report to the General Assembly, United Nations, New York.

- UNSCEAR (2000) Annex B: Exposures from natural radiation sources. United Nations Scientific Committee on the Effects of Atomic Radiation, United States.
- UNSCEAR (2008). Exposure to the public and workers from various sources of radiation. Report to the General Assembly. New York, United Nations, **1**, Annexure B, 234.
- V. Duggal, R. Mehra and A. Rani .Study of Radium and Radon Exhalation Rate in Soil Samples from Areas of Northern Rajasthan. *Journal of Geological Study of India*. (2015);**86(3)**,331-336
- Vanchhawng Lalmuanpuia, Rohmingliana PC, Thapa RK, Sahoo BK, Singh OP, Zoliana B, Mayya YS (2009). To Correlate Radon and Thoron Concentrations with Gamma Background Radiation in Mizoram (Special reference to Aizawl, Champhai and Kolasib districts), Proc. VIth Conference of Physics Academy of North East, Tripura University, April 3-4.
- Verma, D., Khan, M. S., and Zubair, M. (2012). Assessment of effective radium content and radon exhalation rates in soil samples. *J. of Radio. and Nucl. Chem.*, **294(2)**, 267-270.
- Wentworth Chester K (1922). A scale of grade and class terms for clastic sediments. *The Journal of Geology*, **30(5)**, 377-392.
- World Health Organization (2009). Hand Book on Indoor Radon: A public health perspective. Geneva 27, Switzerland: WHO.
- Wrenn ME, Singh NP, Cohen N, Ibrahim SA, Saccomano G (1981). Thorium in Human Tissues. NUREG/CR-1227. Washington, DC: Nuclear Regulatory Commission

**BRIEF BIODATA OF
LALDINGNGHETA RALTE**

Name	:	Laldingngheta Ralte		
Father's Name	:	Lalramhluna		
Date of Birth	:	01 - 02 - 1991		
Address	:	House No. YB-58A, Dawrkawn, Chaltlang, Aizawl, Mizoram, Pin- 796012.		
Subject of Specialization	:	Advanced Electronics		
Educational Qualification	:			
H.S.L.C	:	2007	Distinction	M.B.S.E.
H.S.S.L.C.	:	2009	Second Division	M.B.S.E.
B.Sc. (Physics)	:	2013	Second Division	M.Z.U.
M.Sc. (Physics)	:	2015	First Division	M.Z.U.
Pre-Ph.D Course	:	2016	First Division	M.Z.U.

Working Experience:

- Completed M.Sc. Project work entitled “Study and analysis of mobile signal strength in Chaltlang Area of Aizawl City” at Department of Physics, Mizoram University, Mizoram (796004), 2015.
- Completed training course on workshop entitled, “Measurement techniques for radon, thoron and their decay products”, at Radiological Physics and Advisory Division, Bhabha Atomic Research Centre, Mumbai, during December 13-16, 2016.

- Completed research works on DAE-BRNS Sponsored Project entitled, “*Online monitoring of radon exhalation and modeling in fault regions of Aizawl and Kolasib districts of Northern Mizoram*”, from October 2016 - October 2018 under the supervision of Dr. Rosangliana, Department of Physics, Govt. Zirtiri Residential Science College, Aizawl, Mizoram in collaboration with Radiological Physics and Advisory Division, Bhabha Atomic Research Centre, Mumbai, India.

Publications and activities

Journals:

- **Laldingngheta**, Vanramlawma, Hmingchungnunga, LZ Chhangte, R.C Tiwari, Rosangliana, B. Zoliana, B.K. Sahoo, T.K. Agarwal (2018). Measurement of radon exhalation from soil samples in various fault regions of Aizawl district, Mizoram, India. In *Perspective and Trends in the Development of Science Education and Research, Mizoram Science Congress 2018*, Atlantis Press, Paris, France, pp 198-201. **ISBN:978-94-6252-638-9. ISSN 2352-5401.**
- **Laldingngheta Ralte**, Ramesh Chandra Tiwari, Rosangliana Chawngthu, Bijay Kumar Sahoo (2022)."Analysis of Radon Mass Exhalation in Soil Samples from Fault Regions of Kolasib District Mizoram, India", Volume 10, Issue I, *International Journal for Research in Applied Science and Engineering Technology (IJRASET)* Page No: 77-83, **ISSN : 2321-9653.**
- Laldingngheta Ralte, Ramesh Chandra Tiwari , Vanramlawma, Hmingchungnunga, Rosangliana, B.Zoliana, B.K. Sahoo, T.K. Agarwal. "Analysis of Natural Radioactivity of Soil Samples Using NaI (Tl) Detector from Fault Regions of Kolasib, Mizoram, India", *Radiation Protection Dosimetry. (under review)(scopus indexed journal)*
- Laldingngheta Ralte, Ramesh Chandra Tiwari , Rosangliana, Bijay Kumar Sahoo, Tarun Kumar Agarwal. "Measurement and analysis of Radon Concentrations in Soil Gas Along Kurlok Fault Regions of Kolasib District, Mizoram India", *Journal of Earth System Science (under review)(scopus indexed journal)*

Conferences

National:

- Laldingngheta, Vanramlawma, Hmingchungnunga, LZ Chhangte, R.C. Tiwari, Rosangliana, B.Zoliana, B.K. Sahoo, T.K.Agarwal (2017). Measurement of Radon Exhalation from Soil Samples in Various Fault Regions of Aizawl District, Mizoram, India on National Conference on *Solid*

State Nuclear Track Detectors and Their Applications (SSNTDs-20), during October 26-28, 2017. Vidya Vikas Institute of Engineering and Technology, Mysuru. (Oral Presentation)

- Laldingngheta, Vanramlawma, Hmingchungnunga, LZ Chhange, R.C. Tiwari, Rosangliana, B.Zoliana, B.K. Sahoo, T.K. Agarwal (2018). Measurement of Radon Exhalation from Soil Samples in Various Fault Regions of Aizawl District, Mizoram, India. *Mizoram Science Congress 2018*, during October 4-5, 2018, Pachhunga University College, Aizawl. (Oral Presentation)
- **International**
- Laldingngheta Ralte, Ramesh Chandra Tiwari, Vanramlawma, Hmingchungnunga, Rosangliana, B.Zoliana, B.K. Sahoo, T.K. Agarwal (2018). Measurement of Natural Radioactivity using NaI(Tl) Detector in Soil Samples from Fault Regions of Kolasib District, Mizoram, India. *The 12th Annual Convention of ABAP & International Conference on Biodiversity, Environment and human Health: Innovations and Emerging Trends (BEHIET-2018)*, during November 12-14, 2018. Mizoram University, Mizoram. (**Oral Presentation**)
- Laldingngheta Ralte, Ramesh Chandra Tiwari, Vanramlawma, Hmingchungnunga, Rosangliana, B.Zoliana, B.K. Sahoo, T.K. Agarwal (2019). Measurement of Radon Concentrations in Soil Gas Along Kurlok Fault Regions of Kolasib District, Mizoram. *International Conference on Chemistry and Environmental Sustainability (ICCES-2019)*, during February 20-22, 2019. Mizoram University, Mizoram. (**Poster Presentation**)
- Laldingngheta Ralte, Ramesh Chandra Tiwari, Rosangliana, B.K. Sahoo, T.K. Agarwal (2020). Measurement and Analysis of Radon Concentrations in Soil Gas Along Kurlok Fault Regions of Kolasib District, Mizoram India. *International Seminar on Recent Advances in Science and Technology (ISRAST)*, during 16th – 18th November 2020, Mizoram University, Mizoram (**Online presentation**)

Workshop Attended:

- National Workshop on Quantum Science and Technology, **29-31 July 2019**, Pachhunga University College.

PARTICULARS OF THE CANDIDATE

NAME OF THE CANDIDATE : LALDINGNGHETA RALTE
DEGREE : DOCTOR OF PHILOSOPHY
DEPARTMENT : PHYSICS
TITLE OF THESIS : MEASUREMENT OF RADON
EXHALATION AND ITS
MODELING ALONG KURLOK
FAULT REGIONS OF KOLASIB
DISTRICT, MIZORAM
DATE OF ADMISSION : 08.08.2016

APPROVAL OF RESEARCH PROPOSAL

1. DRC : 19.04.2017
2. BOS : 28.04.2017
2. SCHOOL BOARD : 15.05.2017
3. MZU REGISTRATION No. : 1567 of 2009 -10
4. Ph.D REGISTRATION No. : MZU/Ph.D./1003 of
15.05.2017
5. EXTENSION (IF ANY) : NIL

(Prof. ZAITHANZAUVA PACHUAU)

Head,

Department of Physics

ABSTRACT

**MEASUREMENT OF RADON EXHALATION AND ITS
MODELING ALONG KURLOK FAULT REGIONS OF KOLASIB
DISTRICT, MIZORAM**

**AN ABSTRACT SUBMITTED IN PARTIAL FULFILLMENT OF
THE REQUIREMENTS FOR THE DEGREE OF DOCTOR OF
PHILOSOPHY**

LALDINGNGHETA RALTE

MZU REGISTRATION NO: 1567 of 2009-10

Ph.D REGISTRATION NO: MZU/Ph.D/1003 of 15.05.2017



DEPARTMENT OF PHYSICS

SCHOOL OF PHYSICAL SCIENCE

SEPTEMBER, 2022

**MEASUREMENT OF RADON EXHALATION AND ITS MODELING
ALONG KURLOK FAULT REGIONS OF KOLASIB DISTRICT, MIZORAM**

By

Laldinggheta Ralte

Department of Physics

Name of Supervisor: Prof. R.C.Tiwari

Name of Joint Supervisor: Dr. Rosangliana

Submitted

**in partial fulfillment of the requirement of the
Degree of Doctor of Philosophy
in Physics of Mizoram University, Aizawl**

ABSTRACT

In order to get baseline data on radon movement along fault regions radon mass exhalation, soil gas concentration and radioactivity studies have been done in Kurlok fault regions of Kolasib District. The sampling areas lie within Kolasib District area of Mizoram with several fault lines spread across the areas. The areas extend from 92° 30' 0'' E to 93° 0' 0'' E longitude and 24° 30' 0'' N to 23° 50' 0'' N latitude. Soil samples were collected from the selected faults and were analyzed using various devices. Scintillation based Smart RnDuo was used for measurement of radon mass exhalation from soil samples. This device was also used to measure radon concentration in soil gas at the site of study. This is done by using the device in portable mode and a soil probe to be inserted on the ground. The soil collected from each region was also measured using a NaI(Tl) detector for activity concentration measurement. Soil type determination was done for each sample using a mechanical sieve shaker. Spot background gamma radiation was measured using survey meter PM 1045 at each sampling site at a height of 1m above the ground.

The measurement of mass exhalation was carried out in 36 different locations of Kolasib district in which the values ranges from 2.3 mBqkg⁻¹hr⁻¹ – 45.7 mBqkg⁻¹hr⁻¹ with an average of 20.42 mBqkg⁻¹hr⁻¹. The results obtained from this are comparable to work done in other regions by other investigators. The results in different regions may vary because rainfall, snowfall, freezing and increase in atmospheric pressure results in decrease of exhalation rate, whereas increase in wind speed and temperature can increase it. Also radon exhalation increases with moisture content up to 8% and starts decreasing if water content is increased further. The measured and calculated values have been compared for modeling purpose. values lies within the range of 4.21 mBq/kg/hr to 31 mBq/kg/hr with an average value of 18.7 mBq/kg/hr and standard deviation of 9.44 mBq/kg/hr. With an average of 1.07, the ratio between estimated and measured values ranges from 0.39 to 3.86. Exhalation rates are influenced by a variety of factors, including porosity, temperature, and humidity

Radon gas concentrations are monitored on the ground at depths of 60 cm, 90 cm, and 120 cm along the Kurlok fault regions. The average values of radon concentration in soil gas at the Kurlok Fault zones were 5.93 kBq/m³ at 120 cm depth, 2.93 kBq/m³ at 90 cm depth, and 0.13 kBq/m³ at 60 cm depth. The average concentration of soil gas in the Kurlok fault zones is higher than in the other districts due to the fact that the Kurlok fault consists of a larger or longer fault line that runs through the intersections. Because radon is dependent on faults for transit through rocks beneath the earth, it is expected to be more concentrated in areas with more faults. And it was observed that the concentration increases with increase in depth and this follows the trend of other investigators.

Soil grain size determination was carried out with a mechanical sieve shaker with different mesh sizes. It was observed that the more than 90% of the grain size distribution falls under 'Sand' and it was observed that all the soil from the study area are of sandy soil.

The radioactive concentrations of ²³⁸U, ²³²Th, and ⁴⁰K were assessed from soil samples collected from the study areas and are done with the help of a 5"x4" Sodium Iodide (NaI) detector doped with thallium (Tl) and analyzed using a personal computer-based 1K Multichannel analyzer GSPEC-SA linked with the detector. The values were found to be in the range of 12 Bq/kg to 58 Bq/kg for ²³⁸U, 34 Bq/kg to 161 Bq/kg for ²³²Th and 175 Bq/kg to 1190 Bq/kg for ⁴⁰K with an average of 37 Bq/kg, 102 Bq/kg and 678 Bq/kg for ²³⁸U, ²³²Th and ⁴⁰K respectively. These values when compared with the worldwide values seem to be slightly higher but are lower than the IAEA (2004) critical values.

The average of Radium equivalent activity was found to be of 237 Bq/kg which does not exceed the safe limit of 370 Bq/kg recommended by UNSCEAR (2000). And the average values of external and internal hazard indices were found to be less than 1, which implies that it does not pose any radiological hazard.

Spot background gamma radiation values lines in the range of 89 nSv/hr to 157 nSv/hr with an average of 117 nSv/hr. These values were a bit higher than values provided by UNSCEAR (2000) but were well within the ranges for India. Correlation

between background gamma level and radium equivalent activity in fault regions of Kolasib District was plotted. A very poor correlation was observed due to the fact that cosmic radiations contribute to the background gamma and only the activity concentration measured from three terrestrial radionuclides is accounted for by the radium equivalent activity.